

## Research report

## Detailed neuronal distribution of GPR3 and its co-expression with EF-hand calcium-binding proteins in the mouse central nervous system

Fumiaki Ikawa<sup>a,b</sup>, Shigeru Tanaka<sup>a,\*</sup>, Kana Harada<sup>a</sup>, Izumi Hide<sup>a</sup>, Hirofumi Maruyama<sup>b</sup>, Norio Sakai<sup>a</sup><sup>a</sup> Department of Molecular and Pharmacological Neuroscience, Graduate School of Biomedical and Health Sciences, Hiroshima University, Hiroshima, Japan<sup>b</sup> Department of Neurology, Graduate School of Biomedical and Health Sciences, Hiroshima University, Hiroshima, Japan

## ARTICLE INFO

## Keywords

GPR3  
EF-hand Ca<sup>2+</sup>-binding proteins  
NECAB2  
Hippocampal CA2  
G<sub>s</sub> protein

## ABSTRACT

The G-protein coupled receptor 3 (GPR3), a member of the class A rhodopsin-type GPR family, constitutively activates G<sub>s</sub> proteins without any ligands. Although there have been several reports concerning the functions of GPR3 in neurons, the physiological roles of GPR3 have not been fully elucidated. To address this issue, we analyzed GPR3 distribution in detail using fluorescence-based X-gal staining in heterozygous *GPR3* knockout/*LacZ* knock-in mice, and further investigated the types of GPR3-expressing neurons using fluorescent double labeling with various EF-hand Ca<sup>2+</sup>-binding proteins. In addition to the previously reported GPR3-expressing areas, we identified GPR3 expression in the basal ganglia and in many nuclei of the cranial nerves, in regions related to olfactory, auditory, emotional, and motor functions. In addition, GPR3 was not only observed in excitatory neurons in layer V of the cerebral cortex, the CA2 region of the hippocampus, and the lateral nucleus of the thalamus, but also in  $\gamma$ -aminobutyric acid (GABA)-ergic interneurons in the cortex, hippocampus, thalamus, striatum, and cerebellum. GPR3 was frequently co-expressed with neuronal Ca<sup>2+</sup>-binding protein 2 (NECAB2) in neurons in various regions of the central nervous system, especially in the hippocampal CA2, medial habenular nucleus, lateral thalamic nucleus, dorsolateral striatum, brainstem, and spinal cord anterior horn. Furthermore, GPR3 also co-localized with NECAB2 at the tips of neurites in differentiated PC12 cells. These results suggest that GPR3 and NECAB2 are highly co-expressed in specific neurons, and that GPR3 may modulate Ca<sup>2+</sup> signaling by interacting with NECAB2 in specific areas of the central nervous system.

## 1. Introduction

G-protein coupled receptors (GPRs) are a large family of the most abundant membrane proteins. Among them, GPR3, GPR6, and GPR12 are members of the class A rhodopsin-like GPR family, and constitutively activate the G<sub>s</sub> protein, resulting in elevated basal levels of intracellular cyclic adenosine monophosphate (cAMP) (Eggerickx et al., 1995). GPR3, along with GPR6 and GPR12, forms a subfamily of con-

stitutively active GPRs that have >50% identity at the amino acid level, and that also have homologous amino acid sequences with the lysophosphatidic acid receptor family, sphingosine-1-phosphate (S1P) receptor family, and cannabinoid receptor family (Kakarala and Jamil, 2014). GPR3, GPR6, and GPR12 are more highly expressed in the brain than in other organs (Tanaka et al., 2007). We have previously investigated the functions of GPR3 in neurons and reported that the neuronal expression of GPR3 is associated with neurite outgrowth

**Abbreviations:** AH, anterior horn; BLA, basolateral amygdala; cAMP, cyclic adenosine monophosphate; CCK, cholecystokinin; CeA, centromedial amygdala; CGL, cerebellar granular layer; CGN, cerebellar granule neuron; CNS, central nervous system; Cu, cuneate nucleus; DARPP, dopamine- and cAMP-regulated neuronal phosphoprotein; DCN, deep cerebellar nucleus; DG, dentate gyrus; DLS, dorsolateral striatum; DRG, dorsal root ganglion.; DS, dorsal striatum; EPL, external plexiform layer; ERK, extracellular signal-regulated kinase; GABA,  $\gamma$ -aminobutyric acid; GCL, granule cell layer; GL, glomerular layer; GPR3, G-protein coupled receptor 3; GPRs, G-protein coupled receptors; IPL, internal plexiform layer; IZ, intermediate zone; LN, lateral nucleus; LRt, lateral reticular nucleus; MCL, mitral cell layer; mdT, midline dorsal thalamus; mGluR, metabotropic glutamate receptor; MGP, medial globus pallidus; MHb, medial habenular nucleus; MSN, medium-sized spiny neuron; NECAB, neuronal Ca<sup>2+</sup>-binding protein; ONL, olfactory nerve layer; PBS, phosphate buffered saline; PCP, purkinje cell protein; PG, periglomerular; PH, posterior horn; RGS, regulator of G protein signaling; RN, reticular nucleus; SG, substantia gelatinosa; SNpc, substantia nigra pars compacta; SNpr, substantia nigra pars reticulata; SO, stratum oriens; SP, stratum pyramidale; SR, stratum radiatum; sSA, superficial short-axon; STEP, striatal-enriched protein tyrosine phosphatase; S1P, sphingosine-1-phosphate; TH, tyrosine hydroxylase; VGAT, vesicular gamma-aminobutyric acid transporter; VTA, ventral tegmental area.

\* Corresponding author: Shigeru Tanaka, Department of Molecular and Pharmacological Neuroscience, Graduate School of Biomedical and Health Sciences, Hiroshima University, Hiroshima, 1-2-3, Kasumi, Minami-ku, Hiroshima 734-8551, Japan.

E-mail address: [tanakamd@hiroshima-u.ac.jp](mailto:tanakamd@hiroshima-u.ac.jp) (S. Tanaka)

<https://doi.org/10.1016/j.brainres.2020.147166>

Received 28 February 2020; Received in revised form 7 October 2020; Accepted 12 October 2020

Available online xxx

0006-8993/© 2020.

(Tanaka et al., 2007), modulation of premature neuronal proliferation during the development of cerebellar neurons (Tanaka et al., 2009), and potential anti-apoptotic functions in response to various apoptotic stimuli (Tanaka et al., 2014). No good antibody is currently available for GPR3; thus, we recently investigated the distribution of GPR3 in the brain using *GPR3* knockout/*LacZ* knock-in mice, where the *GPR3* gene locus is genetically substituted with the  $\beta$ -galactosidase gene, *LacZ*. Promoter activity of GPR3 was high in the medial habenular nucleus, hippocampus, thalamus, and pontine nucleus, and was relatively weak in the striatum, cortex, cerebellum, medulla oblongata, brainstem, and spinal cord (Miyagi et al., 2016). Although it has been reported that neuronal GPR3 expression is related to amyloid-beta production (Thathiah et al., 2009, 2013), emotional-like responses (Valverde et al., 2009), neuropathic pain (Ruiz-Medina et al., 2011), and cocaine reinforcement (Tourino et al., 2012), the physiological functions of GPR3 have not yet been fully elucidated.

To aid in our understanding of the physiological functions of GPR3 in the central nervous system (CNS), we believe it is important to conduct a detailed study of the neuronal subtypes that express GPR3 in the central nervous system (CNS). In the mouse CNS, over 250 putative members of EF-hand  $\text{Ca}^{2+}$ -binding proteins have been identified, and some classical EF-hand  $\text{Ca}^{2+}$ -binding proteins, such as calbindin-D28k, calretinin, and parvalbumin, are widely used markers of cell identity (Girard et al., 2015). Thus, the co-localization of GPR3 with previously well-identified EF-hand  $\text{Ca}^{2+}$ -binding protein markers might be useful to identify the subtypes of GPR3-expressing neurons. However, it has been very difficult to perform such studies in the past because of several limitations. A good antibody to detect GPR3 in the mouse brain is not available; we therefore previously used *GPR3* knockout/*LacZ* knock-in mice in combination with X-gal staining to identify the promoter activity of GPR3 in the brain (Miyagi et al., 2016). Although X-gal staining is a well-known technique to detect  $\beta$ -galactosidase in cells and tissues, it is limited by the poor cell permeability of the reagent and its poor signal intensity. Another important limitation is the difficulty in obtaining double colorimetric staining using antibodies, because the glutaraldehyde treatment used for X-gal staining has an adverse effect during immunostaining. To overcome this problem, we used the fluorescence-based  $\beta$ -galactosidase detection reagent SPiDER- $\beta$ Gal in the *GPR3* knockout/*LacZ* knock-in mouse. SPiDER- $\beta$ Gal is reported to have high cell permeability and the ability to remain inside cells, providing high-resolution fluorescent images at a single-cell level (Doura et al., 2016). In addition, SPiDER- $\beta$ Gal-stained samples can be used for immunostaining, and vice versa. Using this method, we were able to identify GPR3-expressing neurons at high resolution, unlike in previous studies, and could further identify the expression of EF-hand  $\text{Ca}^{2+}$ -binding proteins in GPR3-expressing neurons.

Aside from the classical EF-hand  $\text{Ca}^{2+}$ -binding proteins, NECAB2 is the most attractive candidate to investigate the identity of cells that express GPR3; the distribution of NECAB2 is restricted to the CA2 region in the hippocampus (Gerber et al., 2019; Girard et al., 2015; Zimmermann et al., 2013), where GPR3 is predominantly expressed (Miyagi et al., 2016). Members of the NECAB family (NECAB1–NECAB3) contain a single EF-hand domain motif at the N-terminal and a DUF176 motif at the C-terminal, and both NECAB1 and NECAB2 are primarily expressed in the brain (Sugita et al., 2002). It has been reported that NECAB2 interacts with the adenosine A2A receptor, which is a ligand-dependent G $\alpha$ s protein-coupled receptor, and modulates receptor function to activate the mitogen-activated protein kinase (MAPK) pathway (Canela et al., 2007). Furthermore, NECAB2 has also been shown to associate with metabotropic glutamate receptor type 5 (mGluR5) to activate extracellular signal-regulated kinase (ERK)/MAPK pathways and inositol phosphate accumulation (Canela et al., 2009). In addition, NECAB2 plays a role in neuroprotection in the CA2 region of the hippocampus in response to damage, such as

brain ischemia (Kirino, 1982; Yang et al., 2000) and epilepsy (Sloviter, 1991). This role is attributed to its high endogenous  $\text{Ca}^{2+}$ -buffering capacity (Simons et al., 2009).

In the present study, we conducted a detailed evaluation of the distribution and characterization of GPR3-expressing neurons in various regions of the mouse CNS, using double fluorescent labeling of the classical EF-hand  $\text{Ca}^{2+}$ -binding proteins and NECAB2 in *GPR3* knockout/*LacZ* knock-in mice. We found that GPR3 was expressed in both excitatory and inhibitory neurons in various regions of the CNS. In addition, GPR3-expressing neurons highly co-expressed NECAB2 in the mouse CNS. We also evaluated the intracellular co-localization of GPR3 and NECAB2 in differentiated PC12 cells, and revealed that these two proteins were co-localized at the tips of neurites in these cells.

## 2. Results

### 2.1. Detection of GPR3 promoter activity using fluorescence-based X-gal staining in the mouse CNS

We have previously described GPR3 promoter activity using X-gal staining in *GPR3* knockout/*LacZ* knock-in mice (Miyagi et al., 2016); however, the precise distribution of GPR3 remains elusive. To aid in our understanding of GPR3 function, we examined the distribution of GPR3 in the mouse CNS. We used SPiDER- $\beta$ Gal, a fluorescence-based reagent for detecting  $\beta$ -galactosidase activity, to determine the precise location of GPR3 and its co-expression with several EF-hand  $\text{Ca}^{2+}$  binding proteins. First, we evaluated the specificity of SPiDER- $\beta$ Gal staining of GPR3 promoter activity in the *GPR3* knockout/*LacZ* knock-in mice. GPR3 promoter activity was high in the hippocampus, medial habenular nucleus, cerebral cortex, thalamus, striatum, dorsal and ventral brainstem such as the vestibular nucleus and lateral reticular nucleus, and spinal cord; this is consistent with the distribution previously reported using conventional X-gal staining (Fig. 1A, C–V) (Miyagi et al., 2016). Non-specific fluorescence was observed in the SPiDER- $\beta$ Gal-stained sections from wild-type mice except in the cerebellar Purkinje cells (Fig. 1B, Suppl. 1). GPR3 promoter activity in a single cell could be identified more clearly using SPiDER- $\beta$ Gal than with conventional X-gal staining, and with this method we were able to identify GPR3 promoter activity for the first time in a number of brain regions, such as the olfactory bulb, medial globus pallidus (entopeduncular nucleus), amygdala, superior and inferior colliculi, red nucleus, substantia nigra, trigeminal nucleus, vestibular nucleus, cochlear nucleus, facial nucleus, cuneate nucleus, lateral reticular nucleus, and various regions of the spinal cord (Fig. 1D–V). Thus, we concluded that fluorescence-based X-gal staining is promising for the correct identification of GPR3 distribution in the mouse CNS, with high sensitivity, and might be a useful tool for co-expression analysis with EF-hand  $\text{Ca}^{2+}$  binding proteins.

### 2.2. Distribution and characterization of GPR3-expressing neurons in the mouse CNS

In the CNS, neurons can be roughly divided into excitatory and inhibitory neurons, and further classified into specific neuron subtypes in restricted regions. Recently, classical EF-hand  $\text{Ca}^{2+}$ -binding proteins, such as calbindin, calretinin, and parvalbumin, have been used as markers of neuronal identity (Girard et al., 2015). To aid in identifying the functions of GPR3 in neurons, we aimed to identify subpopulations of GPR3-expressing neurons in the mouse CNS. To do this, we performed double fluorescent labeling of GPR3 with classical EF-hand  $\text{Ca}^{2+}$ -binding proteins in various regions of the CNS. In some specific regions, we also determined double fluorescent labeling of GPR3 with the additional neuronal subtype markers, such as GAD67, cholecystokinin (CCK), NECAB2, and tyrosine hydroxylase (TH). In order to check non-specific binding of secondary antibody, we performed sec-

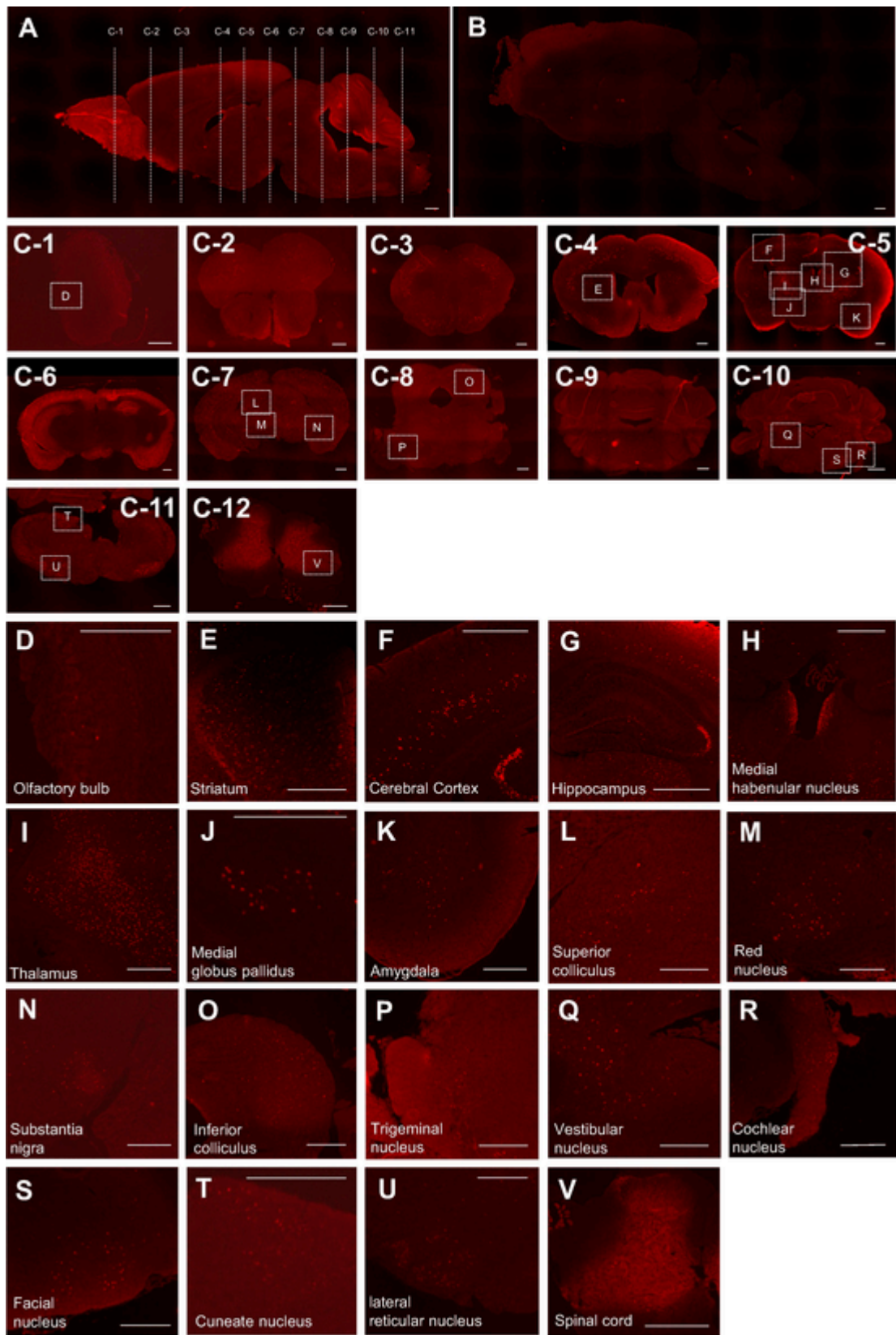


**Fig. 1.** Distribution of GPR3 promoter activity in the mouse CNS using a fluorescence-based X-gal detection system. The promoter activity of GPR3 was investigated using heterozygous *GPR3* knockout/*LacZ* knock-in mice, where the  $\beta$ -galactosidase gene *LacZ* was substituted into the *GPR3* locus. Brain and spinal cord sections were stained with SPiDER- $\beta$ Gal, the fluorescence-based X-gal detection system. The red fluorescence in each section represents cells in which the promoter for GPR3 was activated. Representative sagittal sections (A, B) are shown. Sagittal brain sections from wild-type mice were also stained with SPiDER- $\beta$ Gal as a negative control (B). The representative coronal sections for each location are shown in the sagittal section (A) using dotted lines (C1–C11). The representative coronal sections from the spinal cord are shown in C12. Magnified images of the GPR3-positive areas in coronal sections (en-

closed in dotted squares), where GPR3 promoter activity was relatively high, are shown: olfactory bulb (D), striatum (E), cerebral cortex (F), hippocampus (G), medial habenular nucleus (H), thalamus (I), medial globus pallidus (J), amygdala (K), superior colliculus (L), red nucleus (M), substantia nigra (N), inferior colliculus (O), trigeminal nucleus (P), vestibular nucleus (Q), cochlear nucleus (R), facial nucleus (S), cuneate nucleus (T), lateral reticular nucleus (U), and spinal cord (V). Scale bars = 500  $\mu\text{m}$ . (For interpretation of the references to colour in this figure legend, the reader is referred to the web version of this article.)

ondary antibody alone staining controls for the primary antibodies used throughout (Suppl. 2).

### 2.2.1. Expression patterns of GPR3 in the olfactory bulb

In the olfactory bulb, sparse GPR3 promoter activity was observed in the glomerular layer (GL; Fig. 2A). It has been reported that there are three morphologically distinct types of neurons in the GL: periglomerular (PG) cells (the most common type of neuron in the GL), external tufted (ET) cells, and superficial short-axon (sSA) cells (Nagayama et al., 2014). PG cells can be further classified into two subgroups: TH-positive PG cells (type I) and calbindin- and calretinin-positive PG cells (type II) (Kosaka and Kosaka, 2005). In addition, ET cells were also known to calbindin-positive and calretinin-negative cells, and some ET cells were positive for CCK. GPR3-positive neurons in the GL were almost always positive for calbindin (93.3% of GPR3-expressing cells), and occasionally positive for CCK (30.9% of GPR3-expressing cells) (Fig. 2C–D, G). However, GPR3-positive neurons were not positive for either calretinin or TH (Fig. 2E–F, G). We therefore define that the population of GL neurons that express GPR3 were ET cells, but not PG cells.

### 2.2.2. Expression patterns of GPR3 in the cerebral cortex

The cerebral cortex has a uniform laminar structure and consists of six layers. Calbindin was expressed in neurons in layers II, III, and V of the mouse cortex, which is consistent with previous reports of the rat cortex (Celio, 1990) and mouse visual cortex (Park et al., 2002). In addition, NECAB2 was highly expressed in layers II, IV, and VI (Fig. 3D). Using the expression of these marker proteins and Nissl staining as cortical layers' landmarks, GPR3 promoter activity was observed in layers II, III, IV, V, and VI, with relatively abundant expression in layer V of both the mouse somatosensory and motor cortex (Fig. 3A–B, I–J). Calbindin-positive excitatory neurons and parvalbumin-, somatostatin-, or 5-hydroxytryptamine 3a (5-HT3a) receptor-positive GABAergic interneurons are observed in the cortex (Rudy et al., 2011). To further identify the kinds of GPR3-expressing neurons, we performed double fluorescent labeling of GPR3 with these marker proteins mainly in the somatosensory cortex. In layer V, the GPR3-positive neurons were frequently calbindin-positive (58.9% of GPR3-expressing cells) (Fig. 3C, M) and partially GAD67-positive (26.7% of GPR3-expressing cells) in layer V of somatosensory cortex (Fig. 3E, M). In addition, GPR3-positive neurons were seldom co-localized with parvalbumin-positive neurons (14.4% of GPR3-expressing cells), but not with somatostatin-positive neurons (Fig. 3G–H, M). Moreover, the GPR3-positive neurons were also observed in the GAD67-positive neurons in layer II–IV (36.0% of GPR3-expressing cells) and layer VI (16.7% of GPR3-expressing cells) of cortex (Fig. 3N–O). Besides, the GPR3-positive neurons were stained in the relatively large pyramidal neurons with apical dendrites in the area of motor cortex (Fig. 3L). These cells were highly co-localized with CTIP2 (55.5% of GPR3-expressing cells), which is the maker for corticospinal motor neurons (Fig. 3K, P) [28].

To further identify the subtype of GPR3-expressing neurons in the cortex, we also stained with CCK, which is highly abundant in the basket cells of cerebral cortex (Kawaguchi and Kubota, 1997). Surprisingly, the GPR3-positive neurons were highly expressed in the CCK-positive neurons in all layer of GPR3-expression (67.8% of GPR3-expressing cells in layer V, 47.4% of GPR3-expressing cells in layer II–IV, and 65.2% of GPR3-expressing cells in layer VI, respectively) (Fig. 3F, M–O). Together, these results indicate that GPR3 may abundantly expressed in the CCK-positive excitatory or inhibitory neurons of the adjacent area.

These results suggest that GPR3 is expressed not only in some calbindin-positive excitatory neurons in layer V, but also relatively highly in CCK-positive basket cell in layer II–VI of the mouse cortex.

### 2.2.3. Expression patterns of GPR3 in the hippocampus

In the hippocampus, GPR3 promoter activity was predominantly high in the CA2 area of the pyramidal layer, which is consistent with our previous report (Fig. 4A) (Miyagi et al., 2016). Recently, NECAB2, an EF-hand  $\text{Ca}^{2+}$ -binding protein, has received attention as an anatomical marker of hippocampal CA2 pyramidal neurons (Girard et al., 2015). We therefore determined the double fluorescent labeling of GPR3 and NECAB2, antibody specificity of which was carefully examined by previous report (Zhang et al., 2016). Fluorescent of GPR3 and NECAB2 were exclusively co-localized in the CA2 pyramidal cell layer of Ammon's horn (96.9% of GPR3-expressing cells) (Figs. 4C, 11B, J). These pyramidal neurons generally expressed calbindin (75.2% of GPR3-expressing cells) (Fig. 4D, N), which has been reported to be mainly expressed in excitatory pyramidal neurons in the hippocampus (Jinno and Kosaka, 2002). Thus, GPR3 is expressed in excitatory pyramidal neurons in the CA2 region of the mouse hippocampus.

We also observed a small number of GPR3-positive neurons in the stratum oriens (SO) and stratum radiatum (SR) of Ammon's horn (Fig. 4C–K), as well as in the hilus of the dentate gyrus (DG; Fig. 4L–M). GPR3-positive neurons in these areas were highly co-localized with the inhibitory interneuron marker GAD67 (96.7% of GPR3-expressing cells in CA1 interneuron, 92.0% of GPR3-expressing cells in CA2 interneuron, respectively) (Fig. 4E, I, M–O, Suppl. 3), suggesting that GPR3 is also expressed in inhibitory neurons in the adjacent area of the mouse hippocampus. CCK-positive or parvalbumin-positive GABAergic interneurons have been reported in the SO and SP of Ammon's horn, and basket-type GABAergic neurons are reported to be located in the hilus of the DG (Freund and Buzsaki, 1996; Jinno and Kosaka, 2002; Pelkey et al., 2017; Whissell et al., 2015). Neurons co-expressing GPR3 and CCK were observed highly in the SO of the CA1 (81.0% of GPR3-expressing cells) (Fig. 4J, O) and CA2 (73.3% of GPR3-expressing cells) (Fig. 4F, N), and in the hilus of the DG (63.0% of GPR3-expressing cells) (Fig. 4L, P). Likewise, neurons co-expressing GPR3 and parvalbumin were abundantly observed in the SO of the CA1 (71.0% of GPR3-expressing cells) (Fig. 4K, O) and CA2 (70.4% of GPR3-expressing cells) (Fig. 4G, N), and in the hilus of the DG (21.7% of GPR3-expressing cells) (Fig. 4M, P). Similarly, some somatostatin-positive interneurons were also positive for GPR3 in the SO of the CA2 (57.0% of GPR3-expressing cells) (Fig. 4H, N), but hardly ever co-localized in the CA1 and DG (Fig. 4N, P, Suppl. 3).

These results indicate that GPR3 is mainly expressed in excitatory CA2 pyramidal neurons, but that it is also relatively highly expressed in Parvalbumin-positive or CCK-positive GABAergic interneurons in the CA1, CA2, and DG in the mouse hippocampus.

### 2.2.4. Expression patterns of GPR3 in the thalamus

GPR3 promoter activity was high in the lateral nucleus (LN) region of the thalamus (Fig. 5A). Calretinin-positive neurons were abundant in the midline dorsal thalamus (mdT), but there was no such staining observed in the LN (Giraldez-Perez et al., 2013). The majority of neurons in the LN are glutamatergic excitatory neurons (Fremeau et al., 2004; Giraldez-Perez et al., 2013; Tamamaki et al., 2003). In addition, parvalbumin-positive neurons have been observed in the reticular nucleus (RN) of the rat brain (Arai et al., 1994), but were not observed in the dorsal thalamus in mice (Giraldez-Perez et al., 2013). Furthermore, most neurons in the RN are reported to be

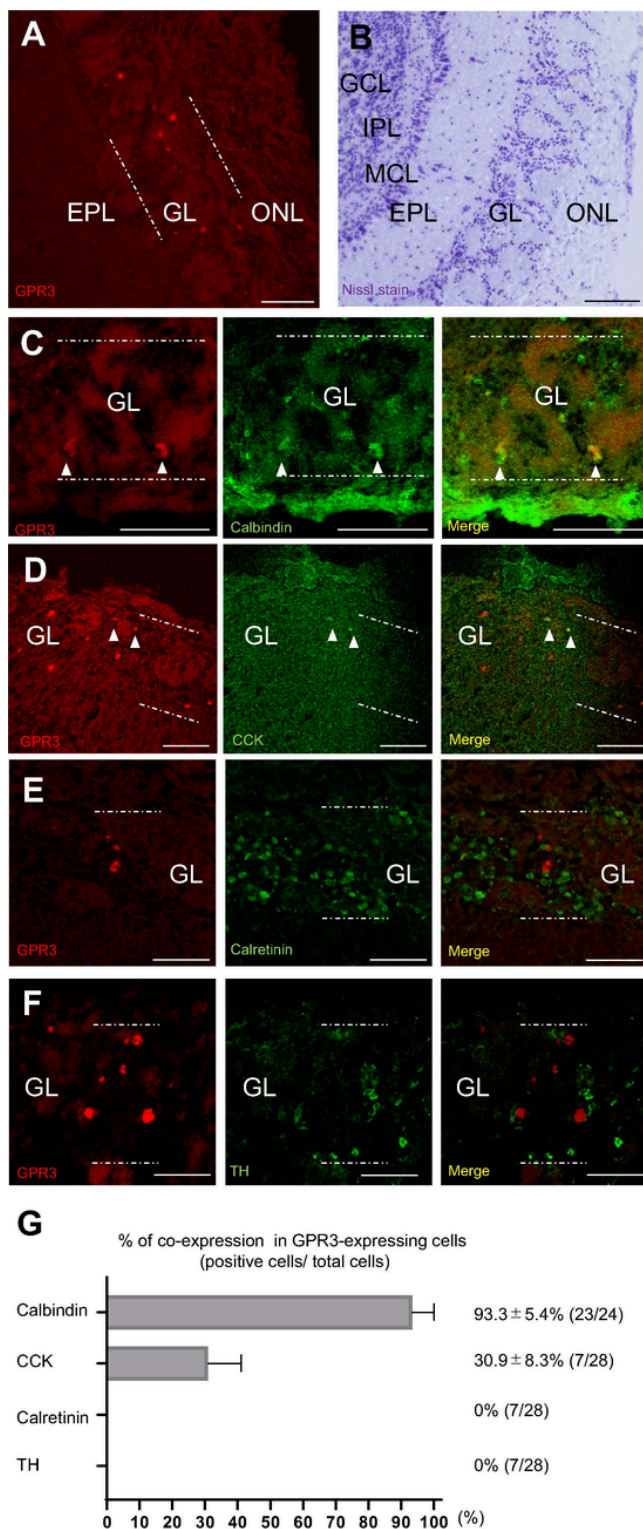


**Fig. 2.** Distribution and characterization of GPR3-positive neurons in the olfactory bulb using double fluorescent labeling in *GPR3* knockout/*LacZ* knock-in mice. Representative images of the olfactory bulb stained with SPiDER- $\beta$ Gal (A) and Nissl (B) in heterozygous *GPR3* knockout/*LacZ* knock-in mice are shown. Double fluorescent labeling of *GPR3* knockout/*LacZ* knock-in mice was performed using antibodies for EF-hand  $Ca^{2+}$ -binding proteins and SPiDER- $\beta$ Gal (for detailed methods see Experimental procedures). Representative images from the double staining of GPR3 with calbindin (C), CCK (D), calretinin (E), and TH (F) are shown. The percentage of GPR3-expressing cells that also expressed each marker in the olfactory bulb was calculated (G). Data represent the % expression of each marker out of the total number of GPR3-expressing neurons in the olfactory bulb.

The actual number of cells in each region is also shown (double-positive cells/total number of GPR3-positive cells). Data are expressed as the mean  $\pm$  SE ( $n = 3$  mice/group). Scale bars = 100  $\mu$ m.

GABAergic neurons (Giraldez-Perez et al., 2013; Guillery and Harting, 2003; Houser et al., 1980). GPR3 promoter activity was predominantly high in the LN, where calretinin staining was not observed (Fig. 5C). Moreover, GPR3-expressing neurons in the RN was always highly positive in the parvalbumin (93.1% of GPR3-expressing cells) (Fig. 5D–F). These results indicate that, in the thalamus, GPR3 is highly expressed both in the excitatory neurons of the LN and the GABAergic inhibitory neurons of the RN.

#### 2.2.5. Expression patterns of GPR3 in the striatum

GPR3 promoter activity was high in the dorsolateral striatum (DLS; Fig. 6A). It has been reported that striatal neurons are largely GABAergic medium-sized spiny neurons (MSNs), although a small number of GABAergic and cholinergic inhibitory interneurons also exist (Mata-males et al., 2009; Tepper and Bolam, 2004; Yokoi et al., 2019). GPR3-positive neurons in the DLS were exclusively positive for DARP-P32, which is a marker of MSNs (63.9% of GPR3-expressing cells) (Fig. 6C, G). Double fluorescent labeling of GPR3 with markers for GABAergic neurons, such as parvalbumin, somatostatin, and calretinin, revealed that GPR3-positive neurons were scarcely ever co-localized with markers of GABAergic neurons in the DLS (Fig. 6D–G). These results suggest that GPR3 is mainly expressed in GABAergic MSNs and rarely expressed in interneurons in the mouse striatum.

#### 2.2.6. Expression patterns of GPR3 in the substantia nigra

The substantia nigra was anatomically divided into two parts; the pars compacta (SNc) and the pars reticulata (SNpr). Neurons in the SNc express tyrosine hydroxylase (TH), thereby supply dopamine to the striatum. GPR3 promoter activity was high in the lateral part of the SNpr, but not expressed in the SNc or ventral tegmental area (VTA) where TH-positive neurons were distributed (Fig. 7A–C, G–I). In the SNpr, two kinds of neurons exist: parvalbumin-positive neurons and vesicular gamma-aminobutyric acid transporter (VGAT)-positive neurons (Rizzi and Tan, 2019). Double fluorescent labeling of GPR3 with parvalbumin revealed that GPR3 was often expressed in many parvalbumin-positive cells in the SNpr (56.9% of GPR3-expressing cells) (Fig. 7D, J). TH-, Calretinin- or calbindin-positive neurons were scarcely or never detectable in the SNpr (Fig. 7C, E–F, J), which is consistent with previous reports (Liang et al., 1996). Thus, GPR3 is highly expressed in parvalbumin-positive neurons in the SNpr, but it remains unknown if GPR3 is also expressed in VGAT-positive neurons in this region.

#### 2.2.7. Expression patterns of GPR3 in the globus pallidus

GPR3 promoter activity was high in the medial region of the globus pallidus (MGP; Fig. 8A, C). We observed that GPR3-positive neurons in MGP were almost always positive for beta-tubulin III and GAD67 (94.8% of GPR3-expressing cells) (Fig. 8C, M, Suppl. 4), which is the markers for inhibitory neurons. It is known that the globus pallidus contains parvalbumin-positive/somatostatin-negative, parvalbumin-negative/somatostatin-positive, and parvalbumin-negative/somatostatin-negative neurons (Miyamoto and Fukuda, 2015). GPR3-positive neurons were largely positive for parvalbumin (81.9% of GPR3-expressing cells) (Fig. 8D, M), but that a small number of GPR3-positive neurons was also positive for somatostatin (12.3% of GPR3-expressing cells) in the examined area (coronal sections, approximately  $-1.5$  mm from bregma) of MGP (Fig. 8E, M). Conversely, GPR3-positive neurons were never positive for calbindin in MGP (Fig. 8F, M). Thus, GPR3 is mainly expressed in parvalbumin-positive inhibitory neurons in the MGP. However, it remains unclear whether GPR3 is also expressed in parvalbumin-negative/somatostatin-negative neurons, because the subpopulations of neurons vary within the MGP.

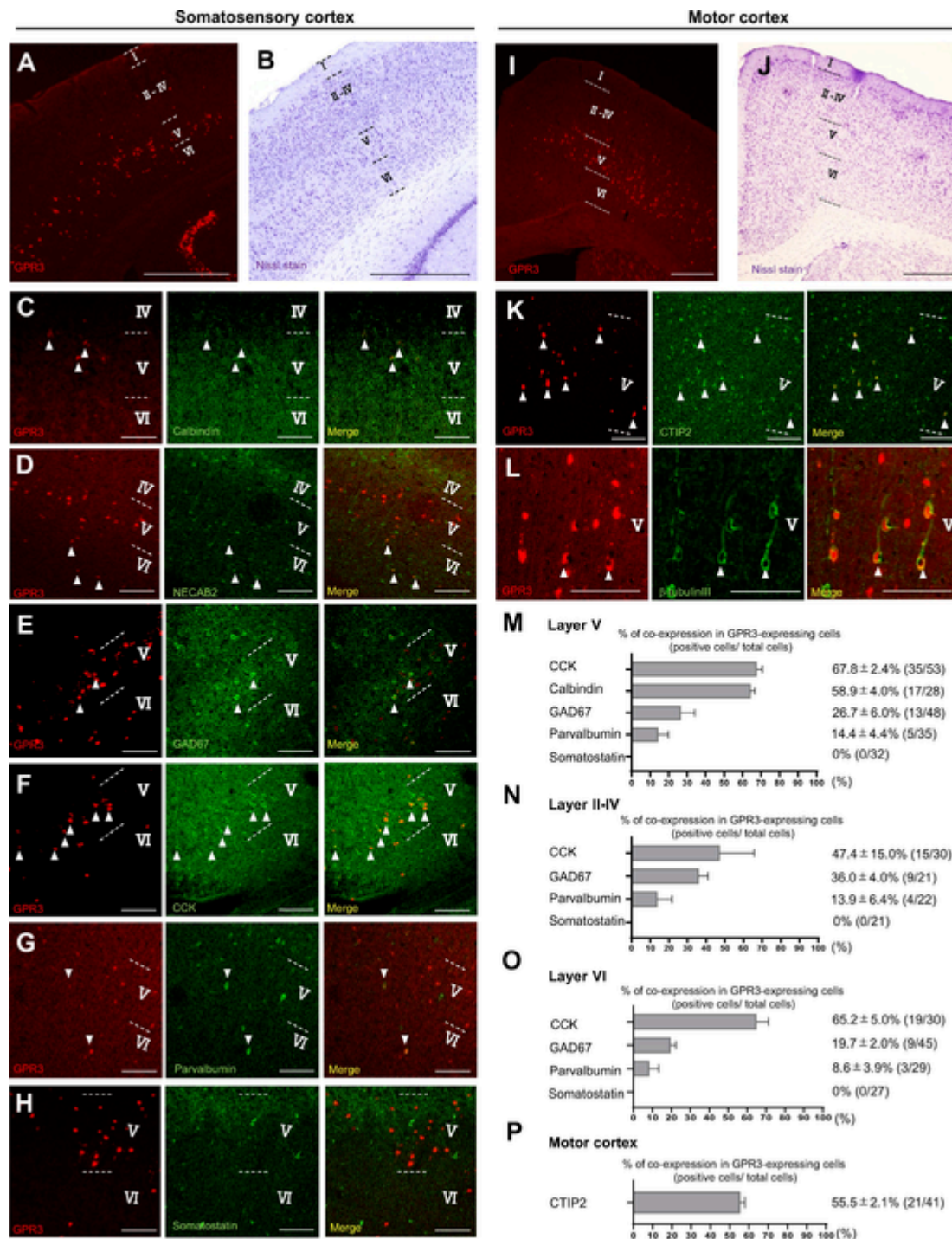


**Fig. 3.** Distribution and characterization of GPR3-positive neurons in the cerebral cortex using double fluorescent labeling in *GPR3* knockout/*LacZ* knock-in mice. Representative images of the cerebral somatosensory and motor cortex stained with SPiDER-βGal (A, I) and Nissl (B, J) in heterozygous *GPR3* knockout/*LacZ* knock-in mice are shown. Double fluorescent labeling of *GPR3* knockout/*LacZ* knock-in mice was performed using antibodies for EF-hand Ca<sup>2+</sup>-binding proteins and SPiDER-βGal. Representative images from the double staining of GPR3 with calbindin (C), NECAB2 (D), GAD67 (E), CCK (F), parvalbumin (G), and somatostatin (H) in the somatosensory cortex. Representative images from the double staining of GPR3 with CTIP2 (K) and β-tubulin III (L) in layers V of the motor cortex are also shown. The fluorescent double-positive neurons are indicated by arrowheads. The superimposed numbers refer to the layers of the cerebral cortex. The percentage of GPR3-expressing cells that also expressed each marker in the somatosensory cortex was calculated in layer V (M), layer II-IV (N), and layer VI (O). The percentage of GPR3-expressing cells that expressed CTIP2 in layer V of the motor cortex was also calculated (P). Data represent the % expression of each marker out of the total number of GPR3-expressing neurons in each layer. The actual number of cells in each region is also shown (double-positive cells/total number of GPR3-positive cells). Data are expressed as the mean ± SE (n = 3 mice/group). Scale bars = 100 μm.

### 2.2.8. Expression patterns of GPR3 in the amygdala

Amygdala nuclei can be divided into three groups: the basolateral amygdala (BLA), cortical-like, and centromedial (CeA) groups (Sah et

al., 2003). The BLA can be further divided into the lateral (LA), basal (BA), and basomedial (BM) nuclei. GPR3-expressing neurons were sparsely observed in the BLA (particularly in the BA and/or BM), and were not observed in the CeA (Fig. 8A, G). Neurons in the BLA are

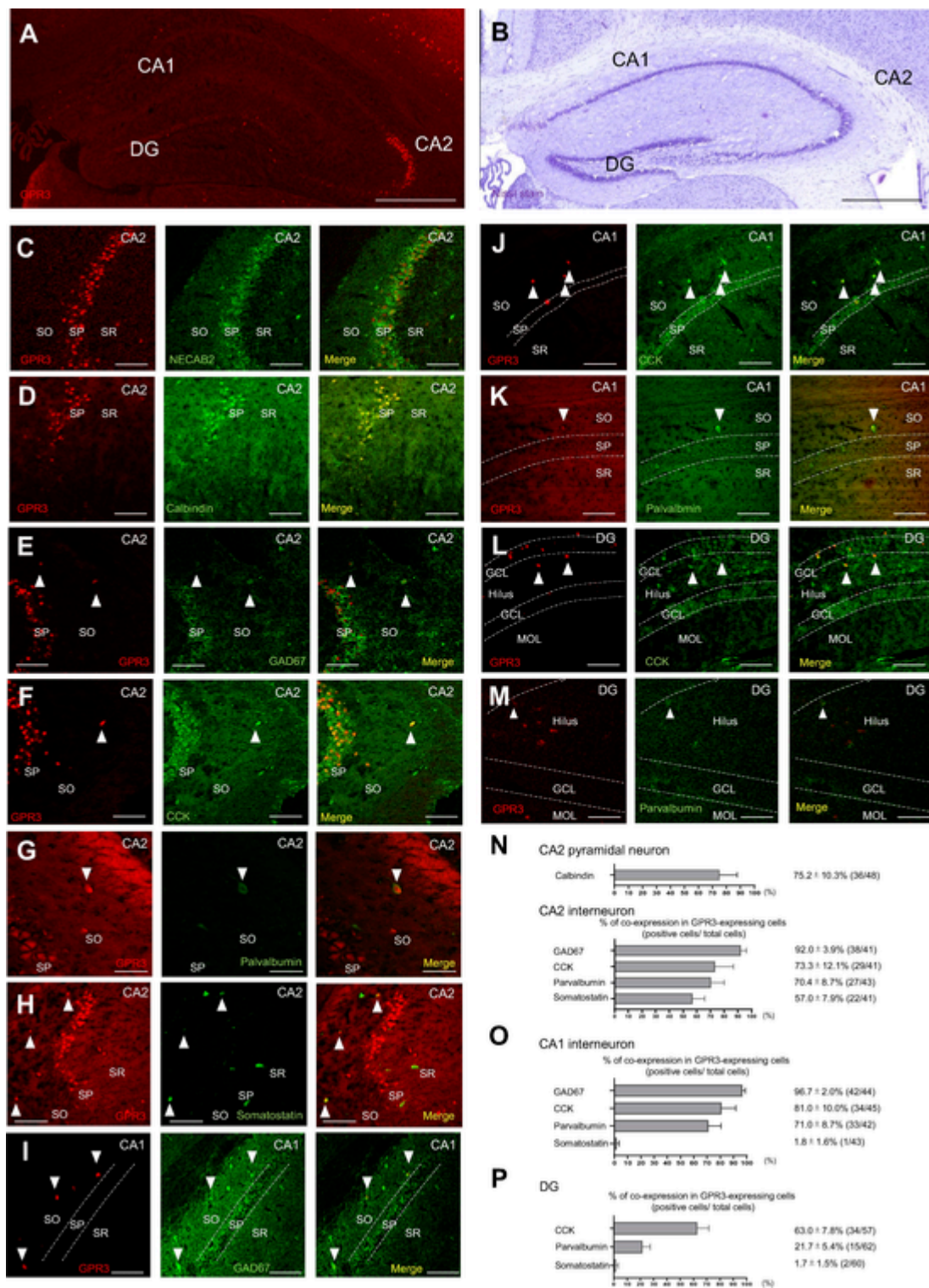


**Fig. 4.** Distribution and characterization of GPR3-positive neurons in the hippocampus using double fluorescent labeling in *GPR3* knockout/*LacZ* knock-in mice. Representative images of the hippocampus stained with SPiDER-βGal (A) and Nissl (B) in heterozygous *GPR3* knockout/*LacZ* knock-in mice are shown. Double fluorescent labeling of *GPR3* knockout/*LacZ* knock-in mice was performed using antibodies for EF-hand  $Ca^{2+}$ -binding proteins and SPiDER-βGal. Representative images from the CA2 region of the hippocampus with double staining of GPR3 with NECAB2 (C), calbindin (D), GAD67 (E), CCK (F), parvalbumin (G) and somatostatin (H) are shown. Representative images from the CA1 region of the hippocampus with double staining of GPR3 with GAD67 (I), CCK (J), and parvalbumin (K) are also shown, as well as from the dentate gyrus of the hippocampus with double staining of GPR3 with CCK (L) and parvalbumin (M). The fluorescent double-positive neurons are indicated by arrowheads. The percentage of GPR3-expressing cells that also expressed each marker in the area of CA2 pyramidal neuron and interneuron (N), CA1 interneuron (O), and DG (P) was calculated. Data represent the % expression of each marker out of the total number of GPR3-expressing neurons. The actual number of cells in each region is also shown (double-positive cells/total number of GPR3-positive cells). Data are expressed as the mean ± SE (n = 3 mice/group). Scale bars = 500 μm (A, B, E, G), 100 μm (C–D, F, H–M).

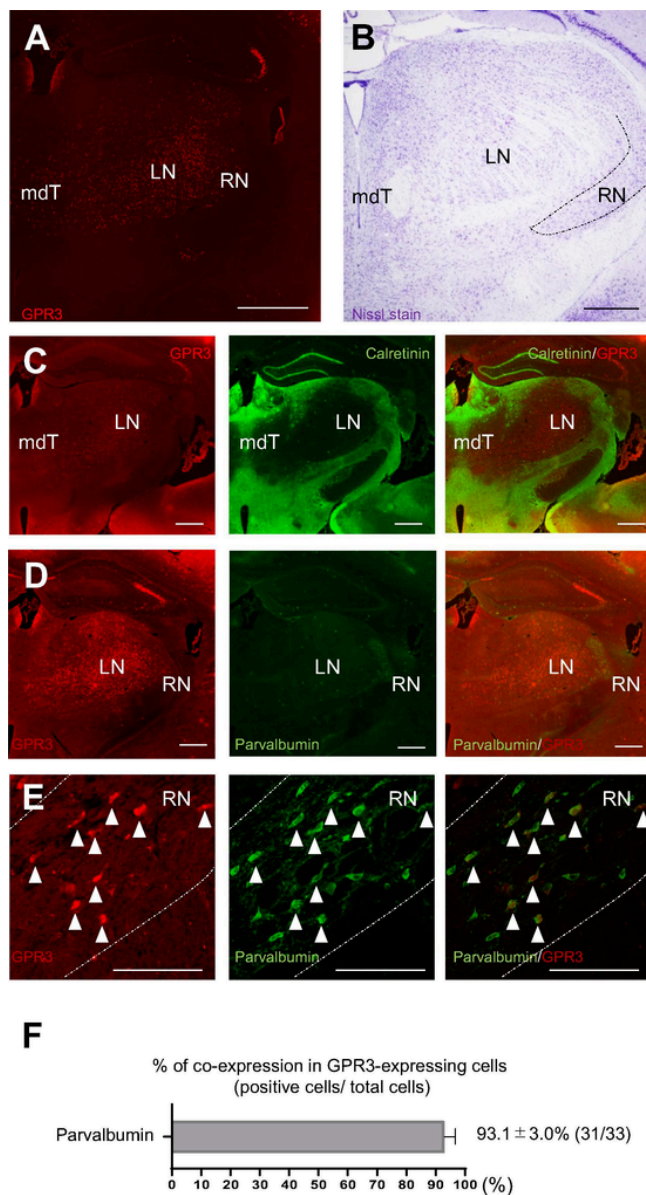


**Fig. 5.** Distribution and characterization of GPR3-positive neurons in the thalamus using double fluorescent labeling in *GPR3* knockout/*LacZ* knock-in mice. Representative images of the thalamus stained with SPiDER-βGal (A) and Nissl (B) in heterozygous *GPR3* knockout/*LacZ* knock-in mice are shown. Double fluorescent labeling of *GPR3* knockout/*LacZ* knock-in mice was performed using antibodies for EF-hand Ca<sup>2+</sup>-binding proteins and SPiDER-βGal. Representative images from the thalamus with double staining of GPR3 with calretinin (C) and parvalbumin (D, E) are shown. The percentage of GPR3-expressing cells that also expressed parvalbumin in the thalamus was calculated (F). Data represent the % expression of each marker out of the total number of GPR3-expressing neurons in the thalamus. The actual number of cells in each region is also shown (double-positive cells/total number of GPR3-positive cells). Data are expressed as the mean ± SE (n = 3 mice/group). Scale bars = 500 μm.

largely glutamatergic neurons (80–85% of all BLA neurons), but a small number of BLA neurons are interneurons (Pape and Pare, 2010; Sah et al., 2003). GPR3-positive neurons in the BLA were exclusively positive for neuronal marker NeuN (Suppl. 4), but rarely positive for GAD67 (24.6% of GPR3-expressing cells) (Fig. 8G, N). These results indicated that GPR3 is not only expressed in GABAergic interneurons, but also be expressed in excitatory glutamatergic neurons in BLA. BLA interneurons can be classified into two groups: calbindin-positive and calretinin-positive interneurons, and Calbindin-positive interneurons further sub-classified into three groups: parvalbumin-positive, somato-

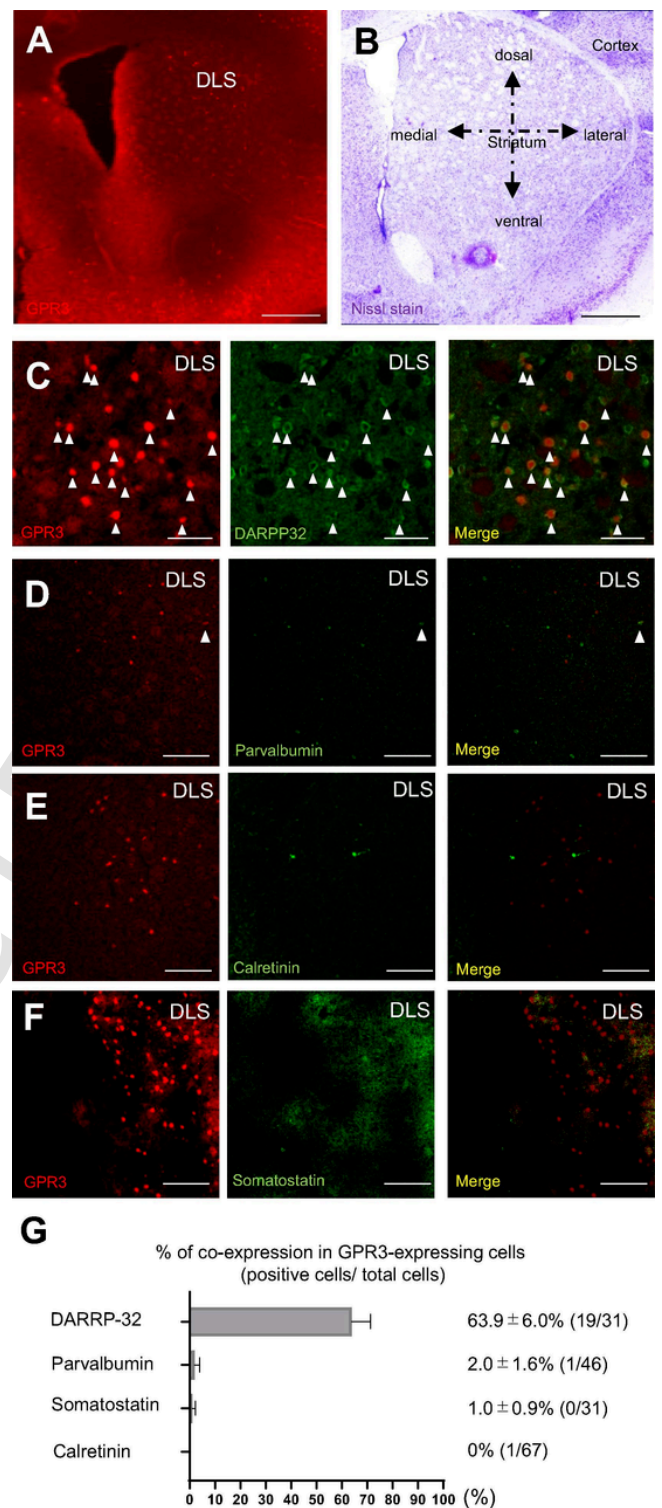


**Fig. 6.** Distribution and characterization of GPR3-positive neurons in the striatum using double fluorescent labeling in *GPR3* knockout/*LacZ* knock-in mice. Representative images of the striatum stained with SPiDER-βGal (A) and Nissl (B) in heterozygous *GPR3* knockout/*LacZ* knock-in mice are shown. Double fluorescent labeling of *GPR3* knockout/*LacZ* knock-in mice was performed using antibodies for EF-hand Ca<sup>2+</sup>-binding proteins and SPiDER-βGal. Representative images from double fluorescent labeling of GPR3 with DARPP32 (C), parvalbumin (D), calretinin (E), and somatostatin (F) in the DLS are shown. The percentage of GPR3-expressing cells that also expressed each marker in the striatum was calculated (G). Data represent the % expression of each marker out of the total number of GPR3-expressing neurons in the striatum. The actual number of cells in each region is also shown (double-positive cells/total number of GPR3-positive cells). Data are ex-

pressed as the mean  $\pm$  SE ( $n = 3$  mice/group). Scale bars = 500  $\mu$ m (A, B), 100  $\mu$ m (C–F).

statin-positive, CCK-positive (Spampanato et al., 2011). GPR3-positive neurons in the BLA were occasionally positive for CCK (37.0% of GPR3-expressing cells), and seldom positive for calbindin (17.4% of GPR3-expressing cells) or parvalbumin (11.7% of GPR3-expressing cells) (Fig. 8H–J, N). GPR3-positive neurons in the BLA were hardly ever positive for somatostatin (6.5% of GPR3-expressing cells), and never positive for calretinin (Fig. 8K–L, N). Thus, we concluded that GPR3 is relatively highly expressed in Calbindin-positive interneurons of the BLA, which might contain CCK-, parvalbumin- or somatostatin-positive interneurons.

### 2.2.9. Expression patterns of GPR3 in the cerebellum

GPR3 was strongly expressed in the deep cerebellar nucleus (DCN) and weakly expressed in the cerebellar granular layer (CGL) of the cerebellum (Fig. 9A). GPR3 is highly expressed during the development of cerebellar granule neurons (CGNs) (Tanaka et al., 2009), but its expression is much weaker in CGNs by 6–12 months of age. Neurons in the CGL consist of CGNs, Lugaro cells, Golgi cells, and unipolar brush cells; both Lugaro cells and a subpopulation of unipolar brush cells are positive for calretinin in this layer (Bastianelli, 2003; Chung

et al., 2009; Sekerkova et al., 2014). However, these GPR3-expressing neurons did not express calretinin (Fig. 9C). Thus, GPR3-positive cells in the CGL might be Golgi cells and calretinin-negative unipolar brush cells. In the DCN, GPR3 was expressed in relatively large neurons (Fig. 9A), and these GPR3-positive neurons also expressed calretinin (73.3% of GPR3-expressing cells) and parvalbumin (86.5% of GPR3-expressing cells) (Fig. 9D–F). It has been reported that both glutamatergic and GABAergic neurons exist in the DCN (Batini et al., 1992). Considering the large size of GPR3-positive neurons, the majority of GPR3-expressing large neurons in the DCN are probably glutamatergic, although GPR3 expression might also be observed in a small number of GABAergic neurons.

### 2.2.10. Expression patterns of GPR3 in the spinal cord

GPR3 promoter activity was high in neurons of the spinal cord, including in the anterior horn (AH), intermediate zone (IZ), and posterior horn (PH), but was sparse in the substantia gelatinosa (SG; Fig. 10A). It has been reported that calretinin in spinal cord neurons is highly co-localized with NECAB2 (Zhang et al., 2016). GPR3-positive neurons were also positive for calretinin (74.1% of GPR3-expressing cells) (Fig. 10C, E) and the co-localization of GPR3 with NECAB2 in neurons was also relatively high in the adjacent areas (86.0% of GPR3-expressing

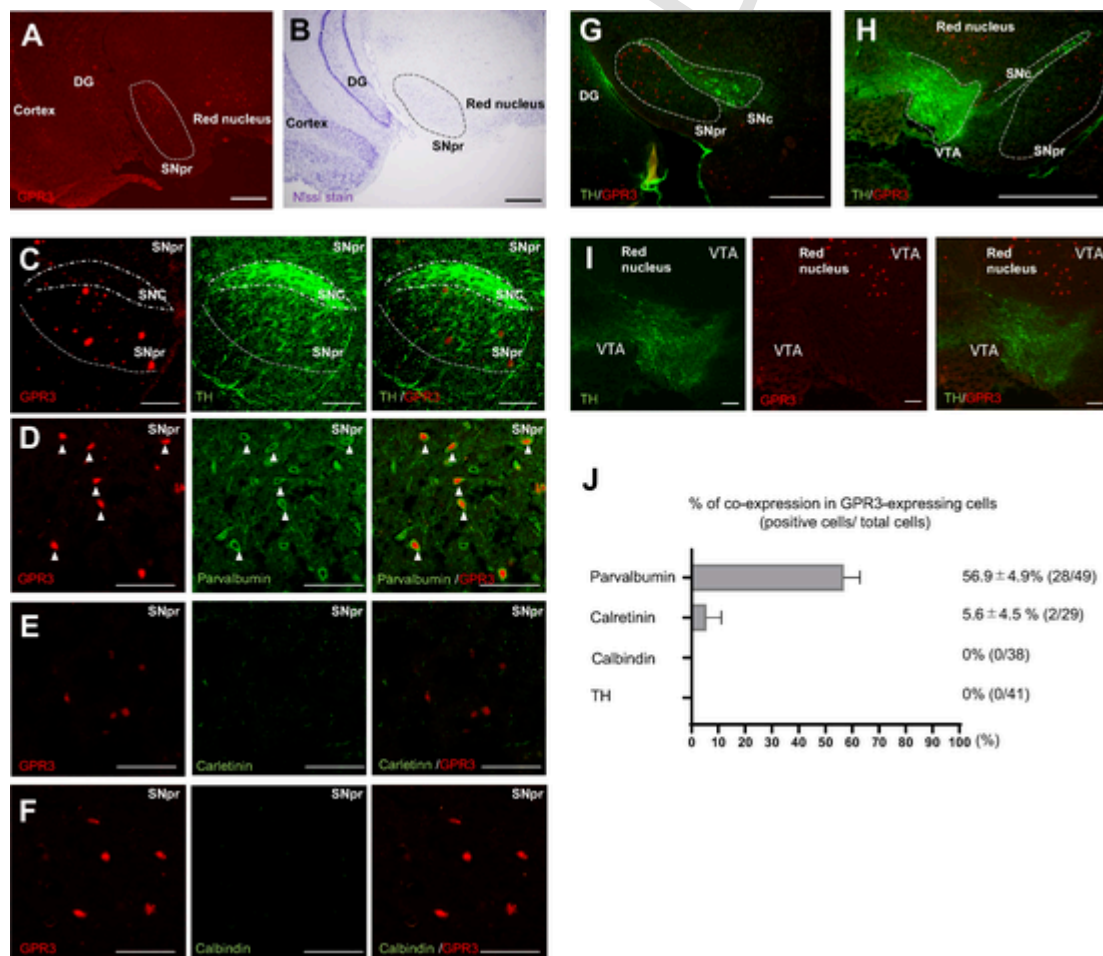


**Fig. 7.** Distribution and characterization of GPR3-positive neurons in the substantia nigra using double fluorescent labeling in *GPR3* knockout/*LacZ* knock-in mice. Representative images of the substantia nigra stained with SPiDER- $\beta$ Gal (A) and Nissl (B) in heterozygous *GPR3* knockout/*LacZ* knock-in mice. Double fluorescent labeling of *GPR3* knockout/*LacZ* knock-in mice was performed using antibodies for EF-hand  $Ca^{2+}$ -binding proteins and SPiDER- $\beta$ Gal. Representative images from double fluorescent labeling of GPR3 with TH (C), parvalbumin (D), calretinin (E), and calbindin (F) in the SNpr and TH (G) in the SNc are shown. Representative images from double fluorescent labeling of GPR3 with TH (H, I) in the VTA are shown. The fluorescent double-positive neurons are indicated by arrowheads. The percentage of GPR3-expressing cells that also expressed each marker in the SNpr was calculated (J). Data represent the % expression of each marker out of the total number of GPR3-expressing neurons in the SNpr. The actual number of cells in each region is also shown (double-positive cells/total number of GPR3-positive cells). Data are expressed as the mean  $\pm$  SE ( $n = 3$  mice/group). Scale bars = 500  $\mu$ m (A, B, G, H), 100  $\mu$ m (C–F).

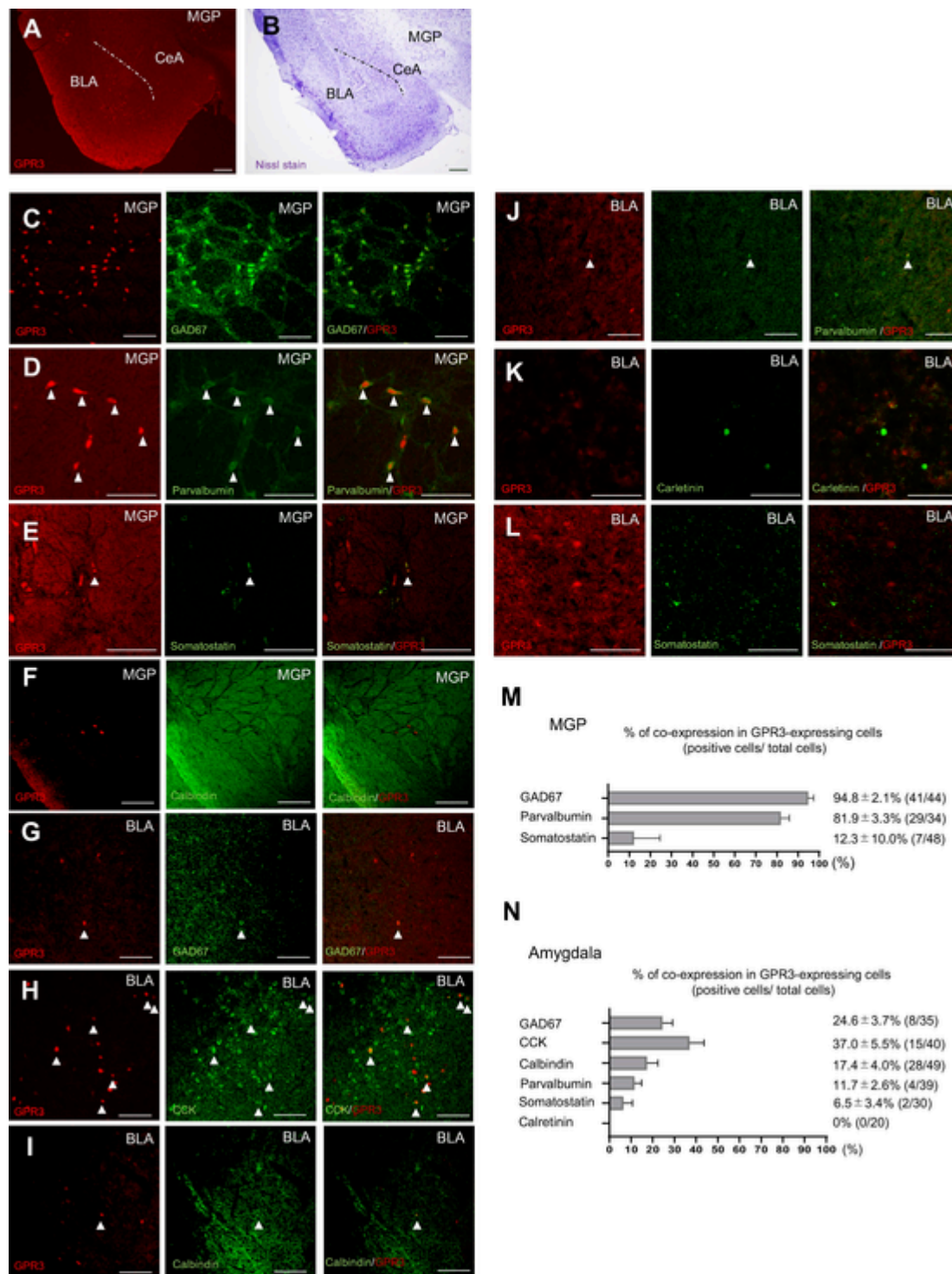


**Fig. 8.** Distribution and characterization of GPR3-positive neurons in the globus pallidus and amygdala using double fluorescent labeling in *GPR3* knockout/*LacZ* knock-in mice. Representative images of the globus pallidus and amygdala stained with SPiDER-βGal (A) and Nissl (B) in heterozygous *GPR3* knockout/*LacZ* knock-in mice. Double fluorescent labeling of *GPR3* knockout/*LacZ* knock-in mice was performed using antibodies for EF-hand Ca<sup>2+</sup>-binding proteins and SPiDER-βGal. Representative images from double fluorescent labeling of GPR3 with GAD67 (C), parvalbumin (D), somatostatin (E), and calbindin (F) in the MGP are shown. Representative images from double fluorescent labeling of GPR3 with GAD67 (G), CCK (H), calbindin (I), parvalbumin (J), calretinin (K), and somatostatin (L) in the BLA are shown. The fluorescent double-positive neurons are indicated by arrowheads. The percentage of GPR3-expressing cells that also expressed each marker in the MGP (M) and BLA (N) was calculated. Data represent the % expression of each marker out of the total number of GPR3-expressing neurons in the MGP and amygdala. The actual number of cells in each region is also shown (double-positive cells/total number of GPR3-positive cells). Data are expressed as the mean ± SE (n = 3 mice/group). Scale bars = 500 μm (A, B), 100 μm (C-L).

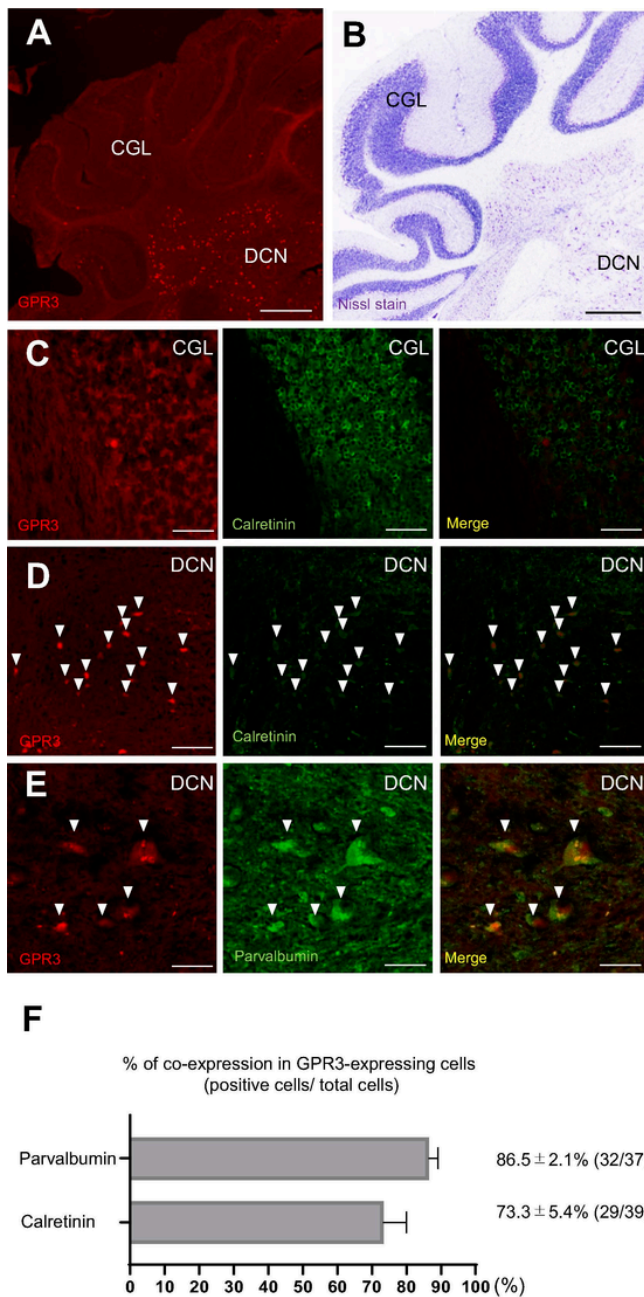


**Fig. 9.** Distribution and characterization of GPR3-positive neurons in the cerebellum using double fluorescent labeling in *GPR3* knockout/*LacZ* knock-in mice. Representative images of the cerebellum stained with SPiDER-βGal (A) and Nissl (B) in heterozygous *GPR3* knockout/*LacZ* knock-in mice. Double fluorescent labeling of *GPR3* knockout/*LacZ* knock-in mice was performed using antibodies for EF-hand  $Ca^{2+}$ -binding proteins and SPiDER-βGal. Representative images from double fluorescent labeling of GPR3 with calretinin (C) in the CGL of the cerebellum, and with calretinin (D) and parvalbumin (E) in the DCN are shown. The fluorescent double-positive neurons are indicated by arrowheads. The percentage of GPR3-expressing cells that also expressed each marker in the DCN of the cerebellum was calculated (F). Data represent the % expression of each marker out of the total number of GPR3-expressing neurons in the DCN of the cerebellum. The actual number of cells in each region is also shown (double-positive cells/total number of GPR3-positive cells). Data are expressed as the mean ± SE (n = 3 mice/group). Scale bars = 500 μm (A, B), 100 μm (C–E).

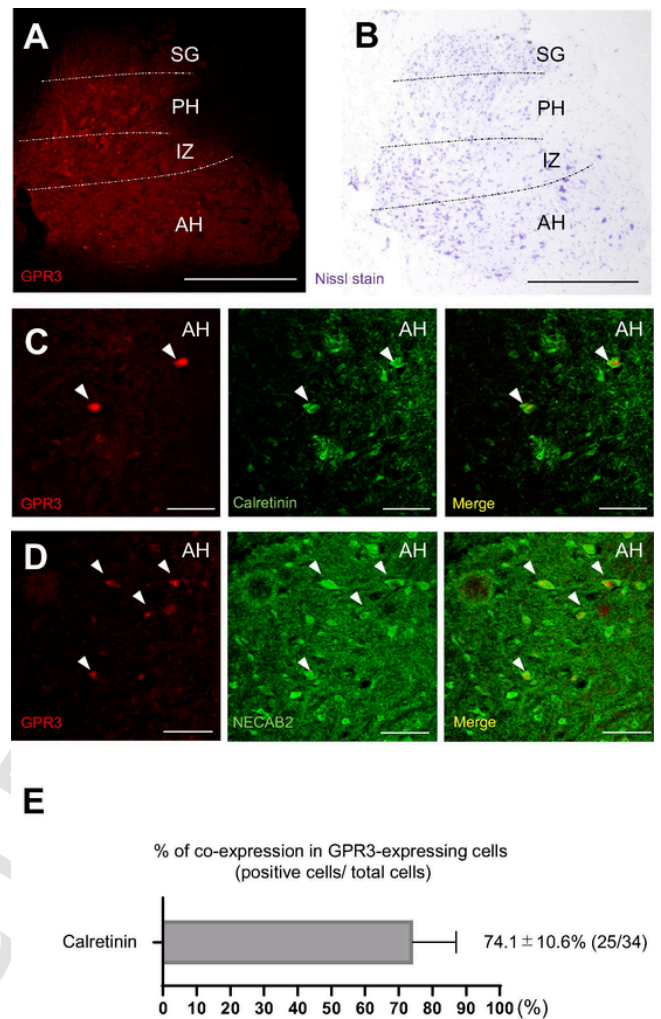


**Fig. 10.** Distribution and characterization of GPR3-positive neurons in the spinal cord using double fluorescent labeling in *GPR3* knockout/*LacZ* knock-in mice. Representative images of the spinal cord stained with SPiDER-βGal (A) and Nissl (B) in heterozygous *GPR3* knockout/*LacZ* knock-in mice. Double fluorescent labeling of *GPR3* knockout/*LacZ* knock-in mice was performed using antibodies for EF-hand  $Ca^{2+}$ -binding proteins and SPiDER-βGal. Representative images from double fluorescent labeling of GPR3 with calretinin (C) and NECAB2 (D) in the AH of the spinal cord are shown. The fluorescent double-positive neurons are indicated by arrowheads. The percentage of GPR3-expressing cells that also expressed calretinin in the spinal cord was calculated (E). Data represent the % expression of calretinin out of the total number of GPR3-expressing neurons in the spinal cord. The actual number of cells in each region is also shown (double-positive cells/total number of GPR3-positive cells). Data are expressed as the mean ± SE (n = 3 mice/group). Scale bars = 500 μm (A, B), 100 μm (C, D).

cells; Figs. 10D, 11I–J). These results indicate that GPR3 is expressed in NECAB2-positive neurons in the AH, IZ, and PH of the spinal cord.

### 2.3. Co-expression of GPR3 with NECAB2 in the mouse CNS

GPR3 and NECAB2 were highly co-localized in the CA2 region of the hippocampus (Fig. 4C). During the course of the current study, we noticed that the distributions of GPR3 were similar to those of NECAB2 in the mouse CNS. We therefore evaluated the percentage of GPR3-expressing neurons that also expressed NECAB2 in various regions of the CNS. NECAB2 was highly expressed in the hippocampus and medial habenular nucleus, and moderately expressed in the cortex, thalamus, striatum, brainstem, and spinal cord (Fig. 11A–J), which is consistent with previous reports (Sugita et al., 2002; Zhang et al., 2016; Zimmermann et al., 2013). Double fluorescent labeling of GPR3 and NECAB2, using *GPR3* knockout/*LacZ* knock-in mice, revealed that

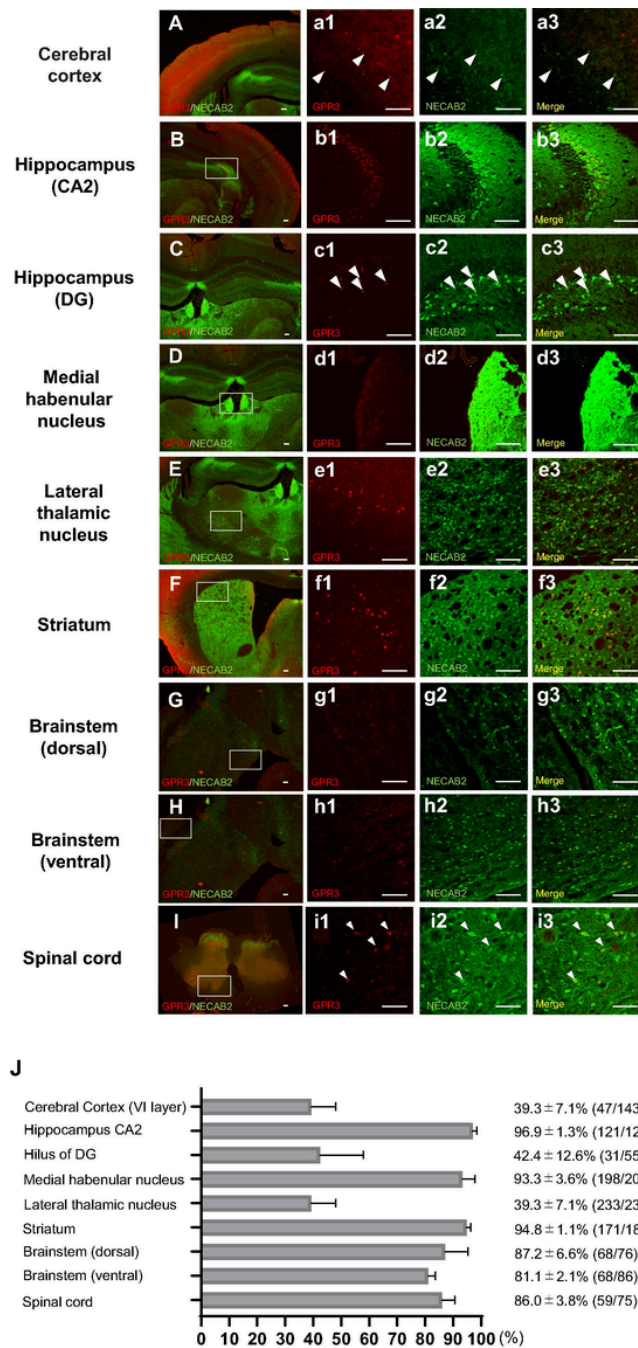


**Fig. 11.** Co-localization of GPR3 with NECAB2 in the mouse CNS. The co-expression of GPR3 and NECAB2 was investigated using fluorescent double staining techniques. Sections from heterozygous *GPR3* knockout/*LacZ* knock-in adult mice were immunostained with NECAB2, followed by fluorescence-based X-gal detection. Representative images of double labeling of GPR3 promoter activity (red) with NECAB2 (green) in the cerebral cortex (A), hippocampus (B, C), medial habenular nucleus (D), lateral thalamic nucleus (E), striatum (F), brainstem (G, H), and spinal cord (I) are shown. High magnification images from each location are also shown (a-i), with GPR3 (red) in a1-i1, NECAB2 (green) in a2-i2, and merged images in a3-i3, respectively. Both GPR3- and NECAB2-expressing neurons are indicated by arrowheads. The percentage of GPR3-expressing cells that also expressed NECAB2 in the mouse CNS was calculated (J). Data represent the % expression of NECAB2 out of the total number of GPR3-expressing neurons in each location. The actual number of cells in each region is also shown (double-positive cells/total number of GPR3-positive cells). Data are expressed as the mean ± SE (n = 3 mice/each location). Scale bars = 100 μm. (For interpretation of the references to colour in this figure legend, the reader is referred to the web version of this article.)

GPR3 and NECAB2 were highly co-expressed in neurons in almost all regions in the CNS, including the hippocampal CA2 (96.9% of GPR3-positive neurons were also NECAB2-positive), medial habenular nucleus (93.3%), dorsolateral striatum (94.8%), dorsal brainstem (87.2%), ventral brainstem (81.1%), and spinal cord anterior horn (86.0%; Fig. 9J). NECAB2 was expressed in a smaller percentage of GPR3-positive neurons in the hilus of the hippocampus (42.4%), layer VI of the cerebral cortex (39.3%), and lateral thalamic nucleus (39.3%). Therefore, NECAB2 was expressed in the majority of GPR3-expressing neurons in the mouse CNS.

#### 2.4. Intracellular co-localization of GPR3 and NECAB2 in cultured neurons

We have shown that NECAB2 was highly expressed in the GPR3-expressing neurons in various regions of the mouse CNS, however these results do not indicate that GPR3 and NECAB2 are co-localized in the intracellular level. We therefore investigated whether or not GPR3 and NECAB2 were co-localized at the intracellular level using cultured neurons. We transfected PC12 cells with pGPR3-mAGFL and evaluated the intracellular co-localization of both proteins. The fluorescence of GPR3 was highly expressed at the tips of neurites at 48 h after differentiation, which is similar to previous findings in cultured CGNs (Fig. 12) (Miyagi et al., 2016). Furthermore, both GPR3 and NECAB2 were highly concentrated and co-localized at the tips of neurites in the differentiated PC12 cells (Fig. 12). These results imply that both GPR3 and NECAB2 are highly co-localized and concentrated at the presynaptic area, and that they may therefore modulate presynaptic functions.

### 3. Discussion

In the present study, we identified the precise regions of GPR3 promoter activity in the mouse CNS using a fluorescence-based X-gal labeling method. We also characterized the different subpopulations of GPR3-expressing neurons using double fluorescent labeling with classical EF-hand  $Ca^{2+}$ -binding proteins, and found that GPR3 was expressed in both excitatory and inhibitory neurons in various regions of the CNS. Finally, we demonstrated that GPR3-expressing neurons were highly co-expressed with NECAB2 in the mouse CNS, and revealed that these two proteins were co-localized at the tips of neurites in differentiated PC12 cells.

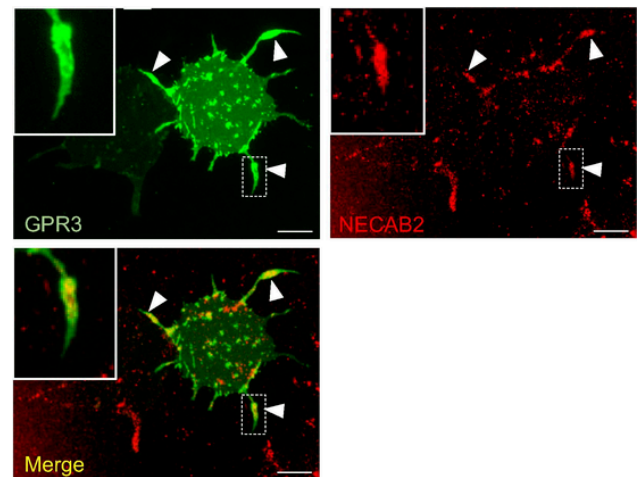


**Fig. 12.** Co-localization of GPR3 with NECAB2 in differentiated PC12 cells. We used a GPR3-GFP expression vector to analyze the localization of GPR3 and NECAB2. At 24 h after the GPR3-GFP vector had been transfected into PC12 cells, differentiation was induced by serum deprivation and NGF addition. At 72 h after transfection, the cells were fixed and immunostained with anti-NECAB2 antibody. A representative image is shown. Left insets are the magnified image of the selected region outlined by the dashed square. GPR3-GFP was highly co-localized with NECAB2 at the tips of neurites in differentiated PC12 cells. Scale bars = 20 μm.

We found that GPR3 was expressed in GABAergic neurons in various regions of the CNS, including the cortex, hippocampus, thalamus, striatum, and cerebellum. However, the functions of GPR3 in GABAergic inhibitory neurons remain unclear. In the hippocampal network, the excitatory glutamatergic neuronal circuit is strongly suppressed by the GABAergic neuronal circuit. The balance between excitation and inhibition is important for proper brain functions, and its disruption leads to aberrant neuronal discharge, which is a hallmark of epilepsy (Dichter and Ayala, 1987). Indeed, it is relatively easy to produce excitatory bursts in neurons of the CA2 and CA3, and this can sometimes cause epilepsy. Moreover, preliminary results from our group have indicated that epilepsy can be induced at lower doses of kainic acid in *GPR3*-knockout mice compared with wild-type mice (unpublished results). The Gs protein-coupled adenosine A2A receptor is also reported to inhibit excitatory neurons by increasing GABA release in inhibitory neurons in the hippocampus (Cunha-Reis et al., 2008) and cerebral cortex (Phillis, 1998). Therefore, the expression of the Gs protein-coupled receptor GPR3 in GABAergic hippocampal neurons may stimulate the release of GABA at basal levels, thereby inhibiting an excitatory burst of glutamatergic neurons in the hippocampus.

During the course of studies, we have noticed that GPR3 was abundantly expressed in CCK-positive excitatory neurons and GABAergic interneurons in various regions of the brain (i.e. olfactory bulb, cerebral cortex, hippocampus, and amygdala). Cannabinoid receptor 1 (CB1), Gi-coupled G-protein coupled receptor, have known to be expressed in the terminal of CCK-positive excitatory neurons and GABA basket interneurons, modulating synaptic function via decreasing levels of intracellular cAMP (Crawford et al., 2011; Eggen et al., 2010). Interestingly, GPR3 and CB1 share similar homology at the amino acid level (Kakarala and Jamil, 2014). Since GPR3 has potential for constitutive activation of intracellular cAMP via Gs-protein, GPR3 and CB1 might play an opposite role in the synaptic functions in the CCK-positive neurons.

We also identified that GPR3 was expressed in excitatory neurons in various brain regions, including layer V of the cerebral cortex, the CA2 region of the hippocampus, and the lateral nucleus of the thalamus. However, the functional role of GPR3 in these neurons is still unclear. We also identified that GPR3 was predominantly expressed in the CA2 hippocampal region, where NECAB2 was also specifically expressed (Gerber et al., 2019; Zhang et al., 2016; Zimmermann et al., 2013). The CA2 region of the hippocampus has recently been re-defined molecularly as the area in which pyramidal neurons receive input from dentate gyrus granule cells and project to the sublayer of CA1 pyramidal neurons (Kohara et al., 2014). Regulator of G-protein signaling 14 (RGS14), Purkinje cell protein 4 (PCP4), striatal-enriched protein tyrosine phosphatase (STEP), and NECAB2 are all used as molecular markers for CA2 (Gerber et al., 2019; Girard et al., 2015; Lee et al., 2010; Lein et al., 2005; Shinohara et al., 2012). Interestingly, the CA2 region of the hippocampus is more resistant to neuronal cell death in response to harmful stimuli compared with other regions of the hippocampus, partly because of the high endogenous  $Ca^{2+}$ -buffering capacity of CA2 neurons, which may related to the expression of NECAB2 (Simons et al., 2009). In addition to the  $Ca^{2+}$ -buffering capacity of NECAB2, recent reports suggest that NECAB2 interacts directly with adenosine A2A receptors to activate their function via the stimulation of Gs-cAMP and MAPK signaling pathways (Canela et al., 2007). Because GPR3 is a Gs-coupled receptor, NECAB2 may also interact with GPR3, stimulating downstream anti-apoptotic signaling and thereby augmenting neuronal survival in response to harmful stimuli in the CA2 region of the hippocampus. In addition to the CA2 region of the hippocampus, GPR3 was also co-expressed with NECAB2 in many other areas of the CNS, including the habenular nucleus, thalamus, striatum, and dorsal region of the brainstem (Fig. 11). Indeed, our previous study indicated that *GPR3*-knockout neurons were more vulnerable to various ischemic-related apoptotic stimuli, and *GPR3*-knockout mice had larger infarcts after transient middle cerebral artery occlusion compared with wild-type mice (Tanaka et al., 2014). Thus, GPR3 may contribute to neuronal survival in regions where GPR3 and NECAB2 are co-expressed. In the present study, we also demonstrated that GPR3 and NECAB2 were highly co-localized at the tips of neurites in PC12 cells. We recently reported that, in CGNs, GPR3 is transported toward neurite tips and contributes to local PKA activation in the adjacent area (Miyagi et al., 2016). The functions of GPR3 in the adjacent areas are still unknown; however, GPR3 may interact with NECAB2 at the tips of neurites, thereby modulating its functions.  $Ca^{2+}$  signaling is very important for neuronal functions such as synaptic transmission and neuronal excitability, and a disruption of  $Ca^{2+}$  homeostasis can lead to neurological diseases, including stroke (Toescu, 2004). It remains elusive whether the co-expression of GPR3 and NECAB2 is necessary for anti-apoptotic and presynaptic functions, and further experiments are needed to clarify the interactions and signaling that occur between NECAB2 and GPR3 in normal and pathological conditions.

Several reports have indicated the association between GPR3 and Alzheimer's disease. GPR3 is involved in the amyloid beta production in neurons in the beta arrestin 2 dependent manner (Thathiah et al., 2009, 2013). In addition, the level of GPR3 expression is elevated in a subset of Alzheimer's disease patients and a lack of GPR3 gene results in a decreased deposition of amyloid plaques and improves the cognitive deficit in Alzheimer's disease mouse model (Huang et al., 2015). These results implicate that the aberrant expression of GPR3 modulates developing the pathogenesis of Alzheimer's disease. However, it is still unclear whether the high expression area of GPR3 in the hippocampus or cortex could modulate the site specific accumulation of senile plaques or neurofibrillary tangle.

We observed the expression of GPR3 in the olfactory bulb, inferior colliculus, cochlear nucleus, and thalamus, which have olfactory and auditory sensory-related functions (Meininger et al., 1986; Pickles, 2015). Likewise, GPR3 expression was observed in the lateral nucleus of the basolateral amygdala and medial habenular nucleus, suggesting that GPR3 may also be related to emotions such as fear and anxiety (Babaev et al., 2018; McLaughlin et al., 2017). Indeed, *GPR3*-knockout mice have been reported to show signs of mood-related disorders such as anxiety, depression-like disorders, and aggressiveness (Valverde et al., 2009). We also identified that GPR3 was highly expressed in the relatively larger pyramidal neurons in cortical layer V of primary motor cortex. Moreover, GPR3 was also expressed in the basal ganglia (i.e., the striatum, substantia nigra, and MGP), red nucleus, DNC, facial nucleus, and vestibular nucleus. Thus, GPR3 may affect motor function and motor refinement. Parvalbumin-positive neurons in the lateral part of the SNpr and in the MGP, and MSNs in the striatum, are thought to be related to the motor initiation dysfunction that occurs in Parkinson's disease (Braak et al., 2004; Rizzi and Tan, 2019). In addition, dysfunction in the basal ganglia causes movement disorders such as Parkinson's and Huntington's diseases (Crittenden and Graybiel, 2011).

In the current study, we identified the specific regions of GPR3-expressing neurons in the mouse CNS. However, it remains unknown whether GPR3 is expressed in the peripheral nervous system. As well as its neuronal expression, GPR3 is also expressed in other regions, such as in oocytes (Mehlmann et al., 2004), testes (Tanaka et al., 2007), and some lymphoid cells (our unpublished results) (Hecker et al., 2011). Clarifying the precise regions of GPR3 expression may help our understanding of the potential functions of GPR3 and the pathophysiology of GPR3-related diseases.

## 4. Experimental procedures

### 4.1. Animals

*GPR3* knockout/*LacZ* knock-in mice with a B6 background were acquired from MMRRC (Bar Harbor, ME, USA) as cryopreserved embryos and were resuscitated at the Institute of Laboratory Animal Science, Hiroshima University, as previously reported (Miyagi et al., 2016; Tanaka et al., 2014). All experiments were approved by the Animal Care and Use Committee, Hiroshima University (approval number A18-105, A18-107).

### 4.2. Fluorescence-based X-gal staining and immunohistochemistry in the mouse CNS

To detect *GPR3* promoter activity, we used the fluorescence-based X-gal staining kit SPiDER- $\beta$ Gal (Fujifilm Wako, Osaka, Japan) on brain sections from heterozygous *GPR3* knockout/*LacZ* knock-in mice. Three male mice of 3–6 months of age were transcardially perfused with ice-cold phosphate buffered saline (PBS) (–) followed by a 4% paraformaldehyde-PBS solution. The brain and spinal cord were then separated and post-fixed with 4% paraformaldehyde-PBS for 4.5–6 h at 4 °C. The specimens were then immersed in 30% sucrose for 3 days and embedded with Tissue-Tek® O.C.T. Compound (Sakura Finetek Japan, Tokyo, Japan). Coronal and sagittal 14  $\mu$ m sections were obtained using a cryostat (Tissue-Tek Polar® DM, Sakura Finetek Japan), mounted on APS-coated slides (Matsunami, Osaka, Japan), and air dried. SPiDER- $\beta$ Gal staining was performed according to the manufacturer's instructions. Briefly, sections were immersed in SPiDER- $\beta$ Gal working solution (SPiDER- $\beta$ Gal substrate diluted in PBS (–) at 1:2000) for 1.5–2 h. The staining reaction was terminated by serial washes with PBS (–). To evaluate the background fluorescence caused by cellular senescence and autofluorescence, sections were taken from age-matched wild-type mice from the same line and genetic background, and SPiDER- $\beta$ Gal staining was evaluated as a negative control in each experiment.

For immunohistochemistry, at least two sections obtained from each mouse were incubated overnight at 4 °C in the following primary antibodies, all diluted at 1:400 in PBS: anti-parvalbumin mouse monoclonal antibody (MAB1572, Merck, Darmstadt, Germany), anti-calretinin rabbit polyclonal antibody (HPA007305, Atlas Antibody, Bromma, Sweden), anti-calbindin mouse monoclonal antibody (C9848, Sigma Aldrich, St. Louis, MO), anti-GAD67 mouse monoclonal antibody (MAB5406, Merck), anti-NECAB2 rabbit polyclonal antibody (HPA013998, Atlas Antibody), anti-tyrosine hydroxylase rabbit polyclonal antibody (AB152, Sigma Aldrich), anti-DARPP32 goat polyclonal antibody (AF6259, R&D Systems, Minneapolis, MN), anti-somatostatin rabbit polyclonal antibody (HPA019472, Atlas Antibody), anti- $\beta$ 3-tubulin rabbit monoclonal antibody (D71G9, Cell Signaling Technology, Danvers, MA), anti-CTIP2 rat monoclonal antibody (25B6, Abcam, Cambridge, UK), anti-cholecystokinin rabbit polyclonal antibody (C2581, Sigma Aldrich), and anti-NeuN mouse monoclonal antibody (MAB377, Sigma Aldrich). After serial washing with PBS (–), sections were immersed in the following secondary antibodies, all diluted at 1:400 in PBS: Alexa Fluor 647-conjugated goat anti-mouse IgG antibody (Thermo Fisher Scientific, Waltham, MA), Alexa Fluor 647-conjugated anti-rabbit IgG antibody (Thermo Fisher Scientific), Alexa Fluor 647-conjugated anti-rat IgG antibody (Abcam), or Alexa Fluor 647-conjugated anti-goat IgG antibody (Abcam). For the double staining of immunohistochemistry sections with X-gal, SPiDER- $\beta$ Gal was used after the immunohistochemical staining protocol.

Stained sections were coverslipped with Mowiol anti-fade mounting media (Merck). Low-magnification images were captured using a BZ-9000 fluorescent microscope (Keyence, Tokyo, Japan) equipped with an oil immersion 60  $\times$  Nikon Plan Apo VC objective lens with a

numerical aperture of 1.4, using 2  $\times$  2 binning and the built-in cooled CCD camera using tile scanning. Images were reconstructed into a single image using a built-in software. For co-localization analysis, double fluorescent images were obtained using a Zeiss 510 or Zeiss 780 confocal microscope (Carl Zeiss, Oberkochen, Germany) and co-localization was analyzed using ImageJ software (<https://imagej.nih.gov/ij/index.html>). For the quantitative analysis, we randomly select *GPR3*-positive cells in the images and counted the number of cells co-expressed with each marker. We calculate the proportion of the co-expression of SPiDER- $\beta$ Gal with each markers, and the number of the proportion quantified was averaged among the three animals. For the co-localization analysis of *GPR3*-expressing cells with NECAB2, at least fifty numbers of neurons were counted in each location and analyzed. All quantitative data are expressed as the mean  $\pm$  SEM with (the number of marker-positive cells/the total counted *GPR3*-positive cells).

### 4.3. Analysis of intracellular NECAB2 distribution in PC12 cells

PC12 cells (a rat pheochromocytoma cell line) were cultured in Dulbecco's modified Eagle medium/F-12 media (1:1; DMEM/F-12) (Fujifilm Wako) supplemented with 10% horse serum (Thermo Fisher Scientific), 5% fetal bovine serum (FBS; Thermo Fisher Scientific), and 1% penicillin streptomycin (Fujifilm Wako). To analyze *GPR3* localization, the monomeric Azami green and FLAG-tagged *GPR3* expression vector (p*GPR3*-mAGFL) (Miyagi et al., 2016) was transfected into cells using a NEPA21 Super Electroporator (Nepa Gene, Chiba, Japan) according to the manufacturer's protocol. Briefly, 5  $\times$  10<sup>6</sup> cells were re-suspended in 100  $\mu$ L of Opti-MEM (Thermo Fisher Scientific) containing 30  $\mu$ g of plasmid DNA, followed by electroporation using a 2 mm gapped cuvette (Napa Gene). Electroporation of the PC12 cells was performed under the following conditions: poring pulse –150 V, 3.0 ms pulse length, 50 ms pulse interval, 2 pulses, 10% decay rate; transfer pulse –20 V, 50 ms pulse length, 50 ms pulse interval, 5 pulses, 40% decay rate. After electroporation, cells were immediately rescued with 600  $\mu$ L of serum-containing culture medium and plated at a density of 7.4  $\times$  10<sup>5</sup> cells per 60 mm tissue culture dish. To induce differentiation, PC12 cells were cultured in DMEM/F-12 (1:1) media supplemented with 1% horse serum, 1% FBS, and 1% penicillin streptomycin for 1 day after the electroporation. On day 2, the cells were fixed with 4% paraformaldehyde. After being blocked with 3% normal goat serum and permeabilized with 0.01% Triton X-100 in PBS (–), cells were incubated overnight at 4 °C with NECAB2 antibody (1:400 in PBS). After serial washing with PBS (–), cells were immersed in Alexa Fluor 647-conjugated goat anti-rabbit IgG antibody (1:400 in PBS) for at least 45 min at 4 °C. After serial washing with PBS (–), co-localization images were taken using a fluorescent microscope.

### Funding

This work was supported by the Ministry of Education, Science, Sports and Culture Grant-in-Aid for Scientific Research (to S.T.) and the Japanese Smoking Research Foundation (to S.T.).

### Author contributions

F.I. and S.T. performed the experiments, analyzed the data and wrote the manuscript. K.H., I.H., H.M., and N.S. supervised the study. All authors contributed to revising the article and approved the final manuscript.

### Declaration of Competing Interest

The authors declare that they have no known competing financial interests or personal relationships that could have appeared to influence the work reported in this paper.

## Acknowledgments

This work was carried out by the joint research program (No. 281022 to S.T.) of Biosignal Research Center, Kobe University. We also wish to thank Dr. Satoshi Tashiro (Research Institute for Radiation Biology and Medicine, Hiroshima University), the Radiation Research Center for Frontier Science and the Natural Science Center for Basic Research and Development, Hiroshima University for the use of their facilities. We also wish to thank Ms. Sasanishi for her excellent technical assistance. We thank Bronwen Gardner, PhD, from Edanz Group (<https://en-author-services.edanzgroup.com/>) for editing a draft of this manuscript.

## Appendix A. Supplementary data

Supplementary data to this article can be found online at <https://doi.org/10.1016/j.brainres.2020.147166>.

## Reference

- Arai, R., Jacobowitz, D.M., Deura, S., 1994. Distribution of calretinin, calbindin-D28k, and parvalbumin in the rat thalamus. *Brain Res. Bull.* 33, 595–614.
- Babae, O., Piletta Chatain, C., Krueger-Burg, D., 2018. Inhibition in the amygdala anxiety circuitry. *Exp. Mol. Med.* 50, 18.
- Bastianelli, E., 2003. Distribution of calcium-binding proteins in the cerebellum. *Cerebellum* 2, 242–262.
- Batini, C., Compoin, C., Buisseret-Delmas, C., Daniel, H., Guegan, M., 1992. Cerebellar nuclei and the nucleocortical projections in the rat: retrograde tracing coupled to GABA and glutamate immunohistochemistry. *J. Comp. Neurol.* 315, 74–84.
- Braak, H., Ghebremedhin, E., Rub, U., Braatzke, H., Del Tredici, K., 2004. Stages in the development of Parkinson's disease-related pathology. *Cell Tissue Res.* 318, 121–134.
- Canela, L., Lujan, R., Lluís, C., Burgueno, J., Mallol, J., Canela, E.I., Franco, R., Ciruela, F., 2007. The neuronal Ca(2+) -binding protein 2 (NECAB2) interacts with the adenosine A(2A) receptor and modulates the cell surface expression and function of the receptor. *Mol. Cell Neurosci.* 36, 1–12.
- Canela, L., Fernandez-Duenas, V., Albergaria, C., Watanabe, M., Lluís, C., Mallol, J., Canela, E.I., Franco, R., Lujan, R., Ciruela, F., 2009. The association of metabotropic glutamate receptor type 5 with the neuronal Ca2+ -binding protein 2 modulates receptor function. *J. Neurochem.* 111, 555–567.
- Celio, M.R., 1990. Calbindin D-28k and parvalbumin in the rat nervous system. *Neuroscience.* 35, 375–475.
- Chung, S.H., Marzban, H., Watanabe, M., Hawkes, R., 2009. Phospholipase Cbeta4 expression identifies a novel subset of unipolar brush cells in the adult mouse cerebellum. *Cerebellum* 8, 267–276.
- Crawford, D.C., Chang, C.Y., Hyrc, K.L., Mennerick, S., 2011. Calcium-independent inhibitory G-protein signaling induces persistent presynaptic muting of hippocampal synapses. *J. Neurosci.* 31, 979–991.
- Crittenden, J.R., Graybiel, A.M., 2011. Basal Ganglia disorders associated with imbalances in the striatal striosome and matrix compartments. *Front. Neuroanat.* 5, 59.
- Cunha-Reis, D., Ribeiro, J.A., Sebastiao, A.M., 2008. A1 and A2A receptor activation by endogenous adenosine is required for VIP enhancement of K+ -evoked [3H]-GABA release from rat hippocampal nerve terminals. *Neurosci. Lett.* 430, 207–212.
- Dichter, M.A., Ayala, G.F., 1987. Cellular mechanisms of epilepsy: a status report. *Science* 237, 157–164.
- Doura, T., Kamiya, M., Obata, F., Yamaguchi, Y., Hiyama, T.Y., Matsuda, T., Fukamizu, A., Noda, M., Miura, M., Urano, Y., 2016. Detection of LacZ-positive cells in living tissue with single-cell resolution. *Angew. Chem. Int. Ed. Engl.* 55, 9620–9624.
- Eggan, S.M., Melchitzky, D.S., Sesack, S.R., Fish, K.N., Lewis, D.A., 2010. Relationship of cannabinoid CB1 receptor and cholecystokinin immunoreactivity in monkey dorsolateral prefrontal cortex. *Neuroscience* 169, 1651–1661.
- Eggerickx, D., Deneff, J.F., Labbe, O., Hayashi, Y., Refetoff, S., Vassart, G., Parmentier, M., Libert, F., 1995. Molecular cloning of an orphan G-protein-coupled receptor that constitutively activates adenylate cyclase. *Biochem. J.* 309 (Pt. 3), 837–843.
- Freneau, R.T., Jr., Voglmaier, S., Seal, R.P., Edwards, R.H., 2004. VGLUTs define subsets of excitatory neurons and suggest novel roles for glutamate. *Trends Neurosci.* 27, 98–103.
- Freund, T.F., Buzsáki, G., 1996. Interneurons of the hippocampus. *Hippocampus.* 6, 347–470.
- Gerber, K.J., Dammer, E.B., Duong, D.M., Deng, Q., Dudek, S.M., Seyfried, N.T., Hepler, J.R., 2019. Specific proteomes of hippocampal regions CA2 and CA1 reveal proteins linked to the unique physiology of area CA2. *J. Proteome Res.* 18, 2571–2584.
- Giraldez-Perez, R.M., Avila, M.N., Feijoo-Cuaresma, M., Heredia, R., De Diego-Otero, Y., Real, M.A., Guirado, S., 2013. Males but not females show differences in calbindin immunoreactivity in the dorsal thalamus of the mouse model of fragile X syndrome. *J. Comp. Neurol.* 521, 894–911.
- Girard, F., Venail, J., Schwaller, B., Celio, M.R., 2015. The EF-hand Ca(2+) -binding protein super-family: a genome-wide analysis of gene expression patterns in the adult mouse brain. *Neuroscience* 294, 116–155.
- Guillery, R.W., Harting, J.K., 2003. Structure and connections of the thalamic reticular nucleus: Advancing views over half a century. *J. Comp. Neurol.* 463, 360–371.
- Hecker, M., Paap, B.K., Goertsches, R.H., Kandulski, O., Fatum, C., Koczan, D., Hartung, H.P., Thiesen, H.J., Zettl, U.K., 2011. Reassessment of blood gene expression markers for the prognosis of relapsing-remitting multiple sclerosis. *PLoS One* 6, e29648.
- Houser, C.R., Vaughn, J.E., Barber, R.P., Roberts, E., 1980. GABA neurons are the major cell type of the nucleus reticularis thalami. *Brain Res.* 200, 341–354.
- Huang, Y., Skwarek-Maruszewska, A., Horre, K., Vandeweyer, E., Wolfs, L., Snellinx, A., Saito, T., Radaelli, E., Corthout, N., Colombelli, J., Lo, A.C., Van Aerscht, L., Callaerts-Vegh, Z., Trabzuni, D., Bossers, K., Verhaagen, J., Ryten, M., Munck, S., D'Hooge, R., Swaab, D.F., Hardy, J., Saïdo, T.C., De Strooper, B., Thathiah, A., 2015. Loss of GPR3 reduces the amyloid plaque burden and improves memory in Alzheimer's disease mouse models. *Sci. Transl. Med.* 7, 309ra164.
- Jinno, S., Kosaka, T., 2002. Patterns of expression of calcium binding proteins and neuronal nitric oxide synthase in different populations of hippocampal GABAergic neurons in mice. *J. Comp. Neurol.* 449, 1–25.
- Kakarala, K.K., Jamil, K., 2014. Sequence-structure based phylogeny of GPCR Class A Rhodopsin receptors. *Mol. Phylogenet. Evol.* 74, 66–96.
- Kawaguchi, Y., Kubota, Y., 1997. GABAergic cell subtypes and their synaptic connections in rat frontal cortex. *Cereb. Cortex.* 7, 476–486.
- Kirino, T., 1982. Delayed neuronal death in the gerbil hippocampus following ischemia. *Brain Res.* 239, 57–69.
- Kohara, K., Pignatelli, M., Rivest, A.J., Jung, H.Y., Kitamura, T., Suh, J., Frank, D., Kajikawa, K., Mise, N., Obata, Y., Wickersham, I.R., Tonegawa, S., 2014. Cell type-specific genetic and optogenetic tools reveal hippocampal CA2 circuits. *Nat. Neurosci.* 17, 269–279.
- Kosaka, K., Kosaka, T., 2005. synaptic organization of the glomerulus in the main olfactory bulb: compartments of the glomerulus and heterogeneity of the periglomerular cells. *Anat. Sci. Int.* 80, 80–90.
- Lee, S.E., Simons, S.B., Heldt, S.A., Zhao, M., Schroeder, J.P., Vellano, C.P., Cowan, D.P., Ramineni, S., Yates, C.K., Feng, Y., Smith, Y., Sweatt, J.D., Weinschenker, D., Ressler, K.J., Dudek, S.M., Hepler, J.R., 2010. RGS14 is a natural suppressor of both synaptic plasticity in CA2 neurons and hippocampal-based learning and memory. *Proc. Natl. Acad. Sci. USA* 107, 16994–16998.
- Lein, E.S., Callaway, E.M., Albright, T.D., Gage, F.H., 2005. Redefining the boundaries of the hippocampal CA2 subfield in the mouse using gene expression and 3-dimensional reconstruction. *J. Comp. Neurol.* 485, 1–10.
- Liang, C.L., Sinton, C.M., German, D.C., 1996. Midbrain dopaminergic neurons in the mouse: co-localization with Calbindin-D28K and calretinin. *Neuroscience* 75, 523–533.
- Matamales, M., Bertran-Gonzalez, J., Salomon, L., Degos, B., Deniau, J.M., Valjent, E., Herve, D., Girault, J.A., 2009. Striatal medium-sized spiny neurons: identification by nuclear staining and study of neuronal subpopulations in BAC transgenic mice. *PLoS One* 4, e4770.
- McLaughlin, I., Dani, J.A., De Biasi, M., 2017. The medial habenula and interpeduncular nucleus circuitry is critical in addiction, anxiety, and mood regulation. *J. Neurochem.* 142 (Suppl. 2), 130–143.
- Mehlmann, L.M., Saeki, Y., Tanaka, S., Brennan, T.J., Evskov, A.V., Pendola, F.L., Knowles, B.B., Eppig, J.J., Jaffe, L.A., 2004. The Gs-linked receptor GPR3 maintains meiotic arrest in mammalian oocytes. *Science* 306, 1947–1950.
- Meininger, V., Pol, D., Derer, P., 1986. The inferior colliculus of the mouse. A Nissl and Golgi study. *Neuroscience* 17, 1159–1179.
- Miyagi, T., Tanaka, S., Hide, I., Shirafuji, T., Sakai, N., 2016. The subcellular dynamics of the Gs-linked receptor GPR3 contribute to the local activation of PKA in Cerebellar Granular Neurons. *PLoS One* 11, e0147466.
- Miyamoto, Y., Fukuda, T., 2015. Immunohistochemical study on the neuronal diversity and three-dimensional organization of the mouse entopeduncular nucleus. *Neurosci. Res.* 94, 37–49.
- Nagayama, S., Homma, R., Imamura, F., 2014. Neuronal organization of olfactory bulb circuits. *Front. Neural Circ.* 8, 98.
- Pape, H.C., Pare, D., 2010. Plastic synaptic networks of the amygdala for the acquisition, expression, and extinction of conditioned fear. *Physiol. Rev.* 90, 419–463.
- Park, H.J., Kong, J.H., Kang, Y.S., Park, W.M., Jeong, S.A., Park, S.M., Lim, J.K., Jeon, C.J., 2002. The distribution and morphology of calbindin D28K- and calretinin-immunoreactive neurons in the visual cortex of mouse. *Mol. Cells.* 14, 143–149.
- Pelkey, K.A., Chittajallu, R., Craig, M.T., Tricoire, L., Wester, J.C., McBain, C.J., 2017. Hippocampal GABAergic Inhibitory Interneurons. *Physiol. Rev.* 97, 1619–1747.
- Phillips, J.W., 1998. Inhibitory action of CGS 21680 on cerebral cortical neurons is antagonized by bicuculline and picrotoxin-is GABA involved? *Brain Res.* 807, 193–198.
- Pickles, J.O., 2015. Auditory pathways: anatomy and physiology. *Handb. Clin. Neurol.* 129, 3–25.
- Rizzi, G., Tan, K.R., 2019. Synergistic nigral output pathways shape movement. *Cell Rep.* 27, 2184–2198.e4.
- Rudy, B., Fishell, G., Lee, S., Hjerling-Leffler, J., 2011. Three groups of interneurons account for nearly 100% of neocortical GABAergic neurons. *Dev. Neurobiol.* 71, 45–61.
- Ruiz-Medina, J., Ledent, C., Valverde, O., 2011. GPR3 orphan receptor is involved in neuropathic pain after peripheral nerve injury and regulates morphine-induced antinociception. *Neuropharmacology* 61, 43–50.
- Sah, P., Faber, E.S., Lopez De Armentia, M., Power, J., 2003. The amygdaloid complex: anatomy and physiology. *Physiol. Rev.* 83, 803–834.

- Sekerova, G., Watanabe, M., Martina, M., Mugnaini, E., 2014. Differential distribution of phospholipase C beta isoforms and diacylglycerol kinase-beta in rodents cerebella corroborates the division of unipolar brush cells into two major subtypes. *Brain Struct. Funct.* 219, 719–749.
- Shinohara, Y., Hosoya, A., Yahagi, K., Ferecsko, A.S., Yaguchi, K., Sik, A., Itakura, M., Takahashi, M., Hirase, H., 2012. Hippocampal CA3 and CA2 have distinct bilateral innervation patterns to CA1 in rodents. *Eur. J. Neurosci.* 35, 702–710.
- Simons, S.B., Escobedo, Y., Yasuda, R., Dudek, S.M., 2009. Regional differences in hippocampal calcium handling provide a cellular mechanism for limiting plasticity. *Proc. Natl. Acad. Sci. USA* 106, 14080–14084.
- Sloviter, R.S., 1991. Permanently altered hippocampal structure, excitability, and inhibition after experimental status epilepticus in the rat: the “dormant basket cell” hypothesis and its possible relevance to temporal lobe epilepsy. *Hippocampus* 1, 41–66.
- Spampanato, J., Polepalli, J., Sah, P., 2011. Interneurons in the basolateral amygdala. *Neuropharmacology* 60, 765–773.
- Sugita, S., Ho, A., Sudhof, T.C., 2002. NECABs: a family of neuronal Ca(2+)-binding proteins with an unusual domain structure and a restricted expression pattern. *Neuroscience* 112, 51–63.
- Tamamaki, N., Yanagawa, Y., Tomioka, R., Miyazaki, J., Obata, K., Kaneko, T., 2003. Green fluorescent protein expression and colocalization with calretinin, parvalbumin, and somatostatin in the GAD67-GFP knock-in mouse. *J. Comp. Neurol.* 467, 60–79.
- Tanaka, S., Ishii, K., Kasai, K., Yoon, S.O., Saeki, Y., 2007. Neural expression of G protein-coupled receptors GPR3, GPR6, and GPR12 up-regulates cyclic AMP levels and promotes neurite outgrowth. *J. Biol. Chem.* 282, 10506–10515.
- Tanaka, S., Shaikh, I.M., Chiocca, E.A., Saeki, Y., 2009. The Gs-linked receptor GPR3 inhibits the proliferation of cerebellar granule cells during postnatal development. *PLoS One* 4, e5922.
- Tanaka, S., Miyagi, T., Dohi, E., Seki, T., Hide, I., Sotomaru, Y., Saeki, Y., Antonio Chiocca, E., Matsumoto, M., Sakai, N., 2014. Developmental expression of GPR3 in rodent cerebellar granule neurons is associated with cell survival and protects neurons from various apoptotic stimuli. *Neurobiol. Dis.* 68, 215–227.
- Tepper, J.M., Bolam, J.P., 2004. Functional diversity and specificity of neostriatal interneurons. *Curr. Opin. Neurobiol.* 14, 685–692.
- Thathiah, A., Spittaels, K., Hoffmann, M., Staes, M., Cohen, A., Horre, K., Vanbrabant, M., Coun, F., Baekelandt, V., Delacourte, A., Fischer, D.F., Pollet, D., De Strooper, B., Merchiers, P., 2009. The orphan G protein-coupled receptor 3 modulates amyloid-beta peptide generation in neurons. *Science* 323, 946–951.
- Thathiah, A., Horre, K., Snellinx, A., Vandeweyer, E., Huang, Y., Ciesielska, M., De Kloe, G., Munck, S., De Strooper, B., 2013. beta-arrestin 2 regulates Abeta generation and gamma-secretase activity in Alzheimer's disease. *Nat. Med.* 19, 43–49.
- Toescu, E.C., 2004. Hypoxia sensing and pathways of cytosolic Ca2+ increases. *Cell Calcium* 36, 187–199.
- Tourino, C., Valjent, E., Ruiz-Medina, J., Herve, D., Ledent, C., Valverde, O., 2012. The orphan receptor GPR3 modulates the early phases of cocaine reinforcement. *Br. J. Pharmacol.* 167, 892–904.
- Valverde, O., Celerier, E., Baranyi, M., Vanderhaeghen, P., Maldonado, R., Sperlagh, B., Vassart, G., Ledent, C., 2009. GPR3 receptor, a novel actor in the emotional-like responses. *PLoS One* 4, e4704.
- Whissell, P.D., Cajanding, J.D., Fogel, N., Kim, J.C., 2015. Comparative density of CCK- and PV-GABA cells within the cortex and hippocampus. *Front. Neuroanat.* 9, 124.
- Yang, G., Kitagawa, K., Ohtsuki, T., Kuwabara, K., Mabuchi, T., Yagita, Y., Takazawa, K., Tanaka, S., Yanagihara, T., Hori, M., Matsumoto, M., 2000. Regional difference of neuronal vulnerability in the murine hippocampus after transient forebrain ischemia. *Brain Res.* 870, 195–198.
- Yokoi, F., Oleas, J., Xing, H., Liu, Y., Dexter, K.M., Misztal, C., Gerard, M., Efimenko, I., Lynch, P., Villanueva, M., Alsina, R., Krishnaswamy, S., Vaillancourt, D.E., Li, Y., 2019. Decreased number of striatal cholinergic interneurons and motor deficits in dopamine receptor 2-expressing-cell-specific Dyt1 conditional knockout mice. *Neurobiol. Dis.* 134, 104638.
- Zhang, M.D., Barde, S., Szodorai, E., Josephson, A., Mitsios, N., Watanabe, M., Attems, J., Lubec, G., Kovacs, G.G., Uhlen, M., Mulder, J., Harkany, T., Hofkelt, T., 2016. Comparative anatomical distribution of neuronal calcium-binding protein (NECAB) 1 and -2 in rodent and human spinal cord. *Brain Struct. Funct.* 221, 3803–3823.
- Zimmermann, B., Girard, F., Meszar, Z., Celio, M.R., 2013. Expression of the calcium binding proteins Necab-1,-2 and -3 in the adult mouse hippocampus and dentate gyrus. *Brain Res.* 1528, 1–7.